COMBINED EFFECTS OF OCEAN ACIDIFICATION AND WARMING ON CALCIFICATION RATE AND SKELETAL MORPHOLOGY OF THE CARIBBEAN REEF-BUILDING CORAL *SIDERASTREA SIDEREA*

Kimmaree Menéndez Horvath

A thesis submitted to the faculty of the University of North Carolina at Chapel Hill in partial fulfillment of the requirements for the degree of Master of Science in the Department of Marine Sciences.

Chapel Hill
2014

Approved by:

Justin Ries

Karl Castillo

Adrian Marchetti

ABSTRACT

Kimmaree Menéndez Horvath: Combined effects of ocean acidification and warming on calcification rate and skeletal morphology of the Caribbean reef-building coral *Siderastrea siderea*
(Under the direction of Justin Ries)

Atmospheric pCO_2 is predicted to rise from 400 to 900 ppm by year 2100, causing seawater temperatures to increase by 1-4 °C and pH to decrease by 0.1-0.3. Sixty-day experiments were conducted to investigate the independent and combined impacts of acidification (pCO_2=425/915 ppm) and warming (T=28/32 °C) on calcification rate and skeletal morphology of the tropical scleractinian coral *Siderastrea siderea*. Coral calcification rate was negatively impacted by warming and acidification, with their combined effects yielding the most negative impact. Effects of warming and high-temperature acidification on calcification rate were apparent across both 30-day observational intervals of the experiment, while effects of low-temperature acidification were not apparent until the second observational interval. Corallite height and infilling were negatively impacted by acidification, but not significantly ($p>0.05$) impacted by warming. These results suggest that *S. siderea* will grow more slowly and accrete weaker skeletons in warmer, more acidic oceans predicted for the future.

ACKNOWLEDGEMENTS

This work was support by the NSF Graduate Research Fellowship DGE-1144081, NOAA awards NA11OAR431016 and NA13OAR4310186, and NSF awards OCE-1031995 and OCE-1357665.

Pualani Armstrong is acknowledged for assistance with microscopic imaging of coral skeletons. Travis Courtney is acknowledged for assistance with statistical analyses. Isaac Westfield and Brian Connolly are acknowledged for assistance with analysis of water chemistry. Maite Ghazaleh, Elaine Chow, Kruti Patel, and Blake Elder are acknowledged for assistance with the coral culturing experiments.

To my committee, Justin Ries, Karl Castillo and Adrian Marchetti: I am indebted to you for your guidance and trust in me as a graduate student and scientist. I am truly fortunate to have had the opportunity to learn from you all.

To my family, Chris, Alexander, and Amelia: life as a wife, a mother, and a graduate student is anything but easy. It would not have been possible without your unconditional support, boundless love, and unwavering belief in my dreams. I hope to provide the same in helping you all to follow your own.

To my mother, Maria Bajo Menéndez: in memory of a life so beautifully lived. If dreams could build a staircase and memories a lane, I'd walk right up to heaven and bring you home again.

TABLE OF CONTENTS

LIST OF FIGURES

LIST OF TABLES

1. INTRODUCTION

In May of 2013, the observatory at Mauna Loa recorded a weekly average atmospheric pCO_2 of 400.01 ppm-v (Tans and Keeling, 2013) – the highest recorded pCO_2 in human history. This represents a 43% increase in atmospheric pCO_2 since preindustrial time, where levels were *ca.* 270-280 ppm-v (Keeling, 1960; Neftel *et al.*, 1985; Rahmstorf *et al.*, 2007; Keeling *et al.*, 2009; Etheridge *et al.*, 2012). This increase is primarily the result of the anthropogenic combustion of fossil fuels, deforestation, and cement production (Keeling, 1960; Neftel *et al.*, 1985; Worrell *et al.*, 2001; IPCC, 2007; Rahmstorf *et al.*, 2007; Keeling *et al.*, 2009). The current pCO_2 level is the highest that the Earth has experienced in the last 800,000 years (Luthi *et al.*, 2008; Kump *et al.*, 2009).

The Intergovernmental Panel on Climate Change (IPCC) predicts that atmospheric pCO_2 will continue to increase to between 550 and 950 ppm-v by the end of the 21st century. This is projected to cause sea surface temperatures to rise by 1 to 4 °C (IPCC, 2007b; Eakin *et al.*, 2008; Donner, 2009). The relationship between seawater temperature and calcification rates of scleractinian corals is relatively well established. Rates generally increase up to a coral's thermal optimum, which typically coincides with the coral's average summertime seawater temperature (Coles and Jokiel, 1977). Above this optimum, rates begin to decline due to bleaching (Hoegh-Guldberg, 1999; Hoegh-Guldberg *et al.*, 2007; Castillo *et al.*, 2014).

In one of the first laboratory studies of its kind, Jokiel and Coles (1977) investigated the effect of temperature on the growth rate of three different species of tropical scleractinian corals. They found that coral mortality commenced within a few days of exposure to an elevated

temperature of 32 °C, and that continued exposure to a temperature of just 30 °C caused bleaching, reduced coral calcification rates, and increased coral mortality. A similar experiment by Glynn and D'Croz (1990) showed that colonies of *Pocillopora damicornis* exposed to temperatures above 30 °C resulted in decreased coral fitness and eventual death. As tropical corals are already encroaching upon the thermal limit during the warmest summer months, the rise in surface seawater temperature that is predicted for the end of this century could result in more frequent bleaching events and subsequent reductions in rates of coral calcification.

This conclusion is supported by the results of several coral-coring studies, such as the one by Tanzil *et al.* (2009) which found that the skeletal extension of *Porites lutea* has declined by approximately 23.5% from 1984 to 2005 and that linear extension rate was inversely correlated with seawater temperature. Additional coring studies report that coral growth declines with increasing seawater temperature (Dodge and Lang, 1983; Cooper *et al.*, 2007; De'ath *et al.*, 2009; Cantin *et al.*, 2010). Castillo *et al.* (2012) determined that linear extension rates of forereef colonies of S. siderea on southern portions of the Belize Barrier Reef have declined with the past ca. 30 years of warming, while colonies from backreef and nearshore environments of the reef have remained stable. Carilli *et al.* (2009) showed that the negative impact of thermal stress on rates of skeletal growth for corals off the coasts of Belize and Honduras is exacerbated by local anthropogenic stressors, such as over-fishing, pollution, and coastal development.

Several coring studies, however, suggest that skeletal growth may increase with warming (Nie *et al.*, 1997; Lough and Barnes 2000; McNeil *et al.*, 2004). Gischler and Oschmann (2005) found no correlation between skeletal growth rates for the corals *Montastraea faveolata* and *S. siderea* and instrumental temperature data.

Rising atmospheric pCO_2 has also caused a 0.1 unit decline in seawater pH since the Industrial Revolution, with an additional 0.1-0.3 unit decrease predicted for the end of this century (Caldera and Wickett, 2003; Orr *et al.*, 2005; Raven *et al.*, 2005). As atmospheric CO_2 dissolves in seawater, it forms carbonic acid (H_2CO_3), which dissociates into bicarbonate (HCO_3^-) and hydrogen ions (H^+), resulting in a decrease in seawater pH and available carbonate ions (CO_3^{2-}) (Zeebe & Wolf-Gladrow, 2001). The decreased CO_3^{2-}concentration ($[CO_3^{2-}]$) causes a reduction in the saturation state of seawater with respect to the aragonite mineral (Ω_A) from which corals build their skeletons. In many cases, this has been shown to impair the ability of scleractinian corals (Gattuso *et al.*, 1998; Leclercq *et al.*, 2002; Langdon and Atkinson, 2005; Schneider and Erez, 2006; Jokiel *et al.*, 2008; Ries *et al.*, 2010; Crook *et al.*, 2013; Castillo *et al.*, 2014) as well as other types of marine calcifiers (e.g., Langdon, 2002; Kleypas *et al.*,2006; Hoegh-Guldberg *et al.*, 2007; Fabry *et al.*, 2008; Doney *et al.*, 2009; Ries *et al.*, 2009) to form their calcareous skeletons.

The effect of ocean acidification on scleractinian coral calcification has been explored in a number of recent studies, with results varying by species as well as by experimental design (Table 1). In a controlled laboratory, Krief *et al.* (2010) showed that although the calcification rate of massive *Porites* sp. and *Stylophora pistillata* declined with decreasing seawater pH, specimens in all treatments survived and continued to accrete new skeleton. Ries *et al.* (2010) found that the temperate coral, *Oculina arbuscula*, exhibited a non-linear negative response to elevated pCO_2, with no change in either rate of net calcification or linear extension from 409 ppm-v to 903 ppm-v, but a severe decline in both at 2,856 ppm-v—the only treatment that was undersaturated with respect to aragonite ($\Omega_A < 1$). Nevertheless, corals were able to continue accreting new skeletal material on a net basis under all pCO_2 treatments (409, 606, 903, 2,856

ppm-v). Similarly, an experimental study by Castillo *et al.* (2014) exposed the tropical scleractinian coral, *Siderastrea siderea* (same species investigated in the present study) to pre-industrial (324 ppm-v), near-present-day (477 ppm-v), elevated (604 ppm-v), and extremely elevated (2553 ppm-v) levels of pCO_2. They found that the response of *S. siderea* to CO_2-induced ocean acidification was parabolic in shape, with moderate elevations in pCO_2 (324-604 ppm-v) causing an increase in calcification rates and extreme elevations (604-2553 ppm-v) causing a decrease in calcification rates. As with Krief *et al.* (2010) and Ries *et al.* (2010), Castillo *et al.* (2014) found that even in seawater that was undersaturated with respect to the aragonite mineral ($\Omega_A < 1$), corals were able to continue accreting new skeletal material throughout the 95-day experiment.

In contrast, a field experiment conducted by Crook *et al.* (2013) concluded that the Caribbean reef-building coral, *Porites astreoides*, was unable to acclimate to reduced Ω_A. They predicted that by the year 2065, calcification rates of *P. astreoides* will have declined by *ca.* 15% since the Industrial Revolution. Their findings are consistent with a 4-year mesocosm study that showed a reef-wide linear decrease in calcification rate with decreasing saturation state (Langdon *et al.*, 2000).

Although the impacts of ocean acidification and warming on reef-building corals have been explored, few studies have investigated the combined effects of these stressors on tropical scleractinian coral calcification. Muehllehner and Edmunds (2008) investigated the interactive effects of increased sea surface temperature and pCO_2 on two species of tropical scleractinian coral (*Pocillopora meandrina* and *Porites rus*) and found that a *ca.* 0.4 decrease in pH had a significant negative impact on coral growth at ambient temperatures (27 °C) relative to the control (*ca.* pH 8.2 and 27 °C), while calcification rates for corals grown at the same decreased

pH of 7.8 and elevated temperature (29 °C) remained largely unchanged. The authors acknowledged, however, that the elevated temperature achieved in the study may not have been high enough to exceed the thermal maximum for these species. In a combined field and laboratory experiment, Rodolfo-Metalpa *et al.* (2011) observed that corals lost the ability to calcify on a net basis in waters undersaturated with respect to Ω_A under elevated temperatures (28.5 °C). As both ocean warming and acidification are predicted for the coming centuries, it is important to constrain the combined effects of these two CO_2-induced stressors on coral calcification.

Equally important to understanding the effect of ocean acidification and increased sea surface temperatures on calcification rate is the impact that these stressors will have on coral skeletal development. Although many studies have investigated the rate of calcification for scleractinian corals under elevated temperature and reduced pH, few have quantified the morphological impact that these individual stressors have on coral skeletal morphology. None have investigated the combined effects of warming and acidification on coral morphology.

One such study by Cohen *et al*. (2009) assessed microscopic scale changes to aragonite crystal formation in new recruits of *Favium fragum* in response to elevated seawater pCO_2. Researchers found that juvenile coral exposed to reduced Ω_A caused by a reduction in seawater pH experienced delayed onset of skeletal development and decreased rates of calcification. Systematic changes to the primary morphology of the precipitated aragonite crystals was also observed: the long, thin blades of densely packed aragonite crystals precipitated under normal conditions were replaced by shorter and thicker crystals arranged in loose bundles formed in waters undersaturated in respect to Ω_A. Their findings were consistent with the results of a study by Holcomb *et al*. (2009) that characterized the morphology and composition of abiogenic

aragonites precipitated in artificial seawater of differing pH. This study found that both the micro- and nano-scale morphology of the crystals changed systematically according to the saturation state and pH of the fluid in which they grew. At normal pH, fine, closed spherulites composed of densely packed bundles of long and blade-like crystals formed, while open and coarse spherulites comprised of short and wide aragonite crystals precipitated at low pH. The present study differs from the Cohen study (2009) investigating the effects of seawater pH on skeletal morphology in that the present study (1) investigates the *combined* effects of increased pCO_2 and temperature on coral skeletal morphology, (2) assesses impacts on the corallites of *adult* coral polyps, and (3) is conducted over relatively long timescales (60 d) that permit evaluation of potential acclimatization to the prescribed stressors.

Here, we present the results of 60-day experiments designed to assess the individual and combined effects of IPCC-predicted end-of-century ocean acidification (pCO_2 = 425, 915 ppm-v) and warming (28, 32 °C) on the calcification rate and skeletal morphology of the tropical reef-building scleractinian coral *Siderastrea siderea*–an abundant and widespread reef-builder throughout Caribbean reef systems.

2. Materials and Methods

2.1 Collection and acclimation

Eighteen colonies of *S. siderea* were collected via SCUBA along the Mesoamerican Barrier Reef System (MBRS), approximately 40 km west of the Belize coast, within the Sapodilla Cayes Marine Reserve (16°□06′□09″□N–88°□16′□20″□W and 16°□07′□00″□N–88°□16′□01″□W) in June 2011, in accordance with local, federal, and international regulations. Large (20-30 yr.) *S. siderea* colonies were selected randomly from 4-5 m deep waters of the nearshore (NS), backreef (BR) and forereef (FR) environments of the MBRS. Colonies were collected at a minimum of 0.5 km apart in order to maximize genotypic variability.

*Siderastrea siderea c*olonies were wrapped in sea-water-moistened paper towels and transported by airplane to the University of North Carolina at Chapel Hill, where they were cut into *ca.* 2 cm x 2 cm fragments with a seawater-cooled petrographic trim saw. Individual coral fragments were affixed with cyanoacrylate to acrylic slides and given a unique ID. Fragments were then placed in a 500 L saltwater aquarium system for 30 days to allow for recovery and acclimation to laboratory conditions prior to the start of the experiment.

2.2 Aquarium conditions

Four experimental treatments of two seawater temperatures (*ca.* 28, 32 °C) crossed with two pCO_2 levels (*ca.* 425 ppm-v, 915 ppm-v) were established. The two temperatures were chosen to coincide with the current average annual temperature on the MBRS in Belize (*ca.* 28 °C) and the worst case scenario IPCC projected temperature increase of 4 °C (*ca.* 32 °C). The two pCO_2 treatments were chosen to represent a near present day atmospheric average (*ca.* 425

ppm-v) and a predicted end-of-century level (*ca.* 915 ppm-v). Each of the four treatments was maintained in triplicate 38 L glass aquaria (12 total).

Twelve similarly sized *S. siderea* fragments obtained from coral colonies equitably distributed amongst the three reef zones were transferred to each of the 12 aquaria (144 total fragments). Corals were acclimatized to experimental growth conditions for fourteen days. The temperature of the seawater in the nominal 32°C treatments was incrementally adjusted from 28 °C to 32 °C over the 14 day period to minimize thermal shock to the corals.

Corals were reared in experimental seawater prepared from deionized water and *Instant Ocean Sea Salt* at a salinity of 35.10 ±0.02. Although the trace elemental composition of *Instant Ocean Sea Salt* differs subtly from that of natural seawater, its major and minor elemental composition, as well as its carbonate chemistry, was the most similar to that of natural seawater when compared with eight other commercial sea salt mixes (Atkinson and Bingman, 1998). Seventy percent water changes were performed approximately every 10 days with *ca.* 35 ppt artificial seawater, and deionized water was added as needed to replenish water lost through evaporation. Water changes for all tanks were performed from a 2000 liter batch of artificial seawater to normalize any potential differences in the composition of the artificial sea salt batches.

Seawater in each aquarium was filtered with activated charcoal and polyester fleece throughout the experiment at a rate of 757 L/h. Water circulation within each tank was enhanced with a powerhead (*Maxi-Jet* 400) attached to each aquarium wall. Aquaria were covered with plexiglass lids and cellophane wrap in order to minimize evaporative water loss and gas exchange with the room air.

Aquaria were illuminated with a timer-controlled 4-stage daily light cycle in order to mimic reef-conditions: 12 hours dark (no light) – 1.5 hours dawn (ultra-actinic-blue light) – 10 hours daylight (ultra-actinic-blue light + 96 Watt 10,000K white light + 32 Watt 6500K fluorescent light) – 1.5 hours dusk (ultra-actinic-blue light). The maximum photosynthetically active radiation (PAR) of the daily light cycles was *ca.* 250 µmol photons m^{-2} s^{-1}. Each coral fragment was fed approximately 1.25 g (wet-weight) *Artemia* sp. twice weekly via a 1-ml graduated transfer pipette. *Artemia* sp. were evenly distributed across the surface of each coral fragment.

2.3 Experimental conditions

Seawater temperatures (28.1 ± 0.1 °C and 31.9 ±0.1 °C at *ca.* 425 ppm-v pCO_2; 28.0 ±0.1 °C and 31.8 ±0.1 °C at *ca.* 915ppm-v pCO_2) were maintained with 50 W submersible aquarium heaters affixed to the side of each aquarium, which were calibrated with NIST-traceable glass thermometers.

Aalborg digital solenoid-valve mass flow controllers were used to blend compressed CO_2 gas with compressed air to achieve gas mixtures with pCO_2 levels consistent with the beginning and predicted-end of the 21st century (IPCC, 2007): 426 ±11 ppm-v and 888 ±14 ppm-v at *ca.* 28 °C; 424 ±10 ppm-v and 940 ±10 at *ca.* 32 °C (Table 2). These gas mixtures were delivered to the aquaria via micro-porous ceramic gas bubblers.

2.4 Measured parameters

Seawater temperature, salinity, and pH were measured three times per week throughout the duration of the experiment (Table 2). Temperature was determined with a NIST-calibrated partial-immersion organic-filled glass thermometer. Salinity measurements were made using a *YSI 3200* conductivity meter outfitted with a *YSI 3440* conductivity cell (K=10). This cell was

calibrated with seawater standards of known salinity supplied by the laboratory of Prof. A. Dickson of Scripps Institute of Oceanography. Aquaria pH readings were taken with an *Orion* benchtop pH meter and an *Orion* Ross pH electrode calibrated with 7.00 and 10.01 certified NBS buffers traceable to NIST standard reference material (for slope of the calibration curve) and with seawater standards of known pH provided by the laboratory of Prof. A. Dickson of Scripps Institute of Oceanography (for y-intercept of the calibration curve).

Approximately 250 ml seawater samples were collected weekly from experimental aquaria in accordance with accepted best practices (Riebesell *et al.*, 2010). These samples were analyzed for dissolved inorganic carbon (DIC) and total alkalinity (TA) on a *MARIANDA* corporation *VINDTA 3C*. Seawater DIC was measured via coulometry (*UIC 5400*) and TA was measured via closed-cell potentiometric titration (Table 2).

2.5 Calculated parameters

Seawater pCO_2, pH, carbonate ion concentration ($[CO_3^{2-}]$), bicarbonate ion concentration ($[HCO_3^-]$), aqueous CO_2, and aragonite saturation state (Ω_A) were calculated with the program CO2SYS (Lewis & Wallace, 1998), using Roy *et al.* (1993){Roy, 1993 #125} values for the K_1 and K_2 carbonic acid constants, the Mucci (1983){Mucci, 1983 #126} value for the stoichiometric aragonite solubility product, and an atmospheric pressure of 1.015 atm (Table 2).

2.6 Estimation of coral bleaching

Photographs of each coral specimen were obtained at the onset (time = 0 d), midpoint (time = 30 d), and completion (time = 60 d) of the study for the evaluation of bleaching. Algae and excess moisture were gently removed from the surface of each coral specimen to reduce glare. The specimen was then placed on a grey background and photographed with a red, green, yellow, and cyan reference palette. Images were obtained with a *Canon* digital camera mounted

to a stand, with identical illumination levels, camera settings, and working distances. An observer based reference card (Coral Watch Coral Health Chart, University of Queensland) was used to determine the hue and saturation/brightness value of each specimen by visual comparison of the specimen to the chart. Saturation/brightness values ranged from 6 (maximum saturation/brightness) to 1 (complete loss of pigmentation) on the reference card. The occurrence of bleaching in a given specimen was assessed by comparing the specimen's observed saturation/brightness value between the beginning and end of the experiment (Siebeck *et al.*, 2006). Bleaching was considered to have occurred when a decrease in saturation/brightness value of two or more units was observed.

2.7 Estimation of coral calcification rate

Rate of coral calcification was estimated via the buoyant weight method (see detailed methods in the online supplement to Ries *et al.*, 2009). Weights were recorded at the beginning, middle, and end of the experiment by suspending coral fragments from an aluminum wire affixed to a *Cole Parmer* bottom-loading scale at a depth of *ca.* 10 cm in experimental seawater maintained at 25 °C and 33 ppt (Table 3). An object of known weight was intermittently weighed to verify consistency of the buoyant weighing method throughout the duration of the experiment.

The buoyant weight-dry weight relationship for the coral *S. siderea* was empirically derived by plotting the final dry weights against the final buoyant weights of all coral specimens (Fig. 1 a-b). Final buoyant and dry weights of coral specimens from each of the two sets of pCO_2 treatments (pCO_2 = 425 ppm-v at 28 and 32 ºC; pCO_2 = 915 ppm-v at 28 and 32 ºC) were highly linearly correlated (R^2 = 0.9452 at *ca.* 425 ppm-v and R^2 = 0.9973 at *ca.* 915 ppm-v),

indicating that linear equations could be used to convert buoyant weight to dry weight for the purposes of estimating calcification rates:

425 ppm-v: Dry weight (mg) = 1579.7 (Buoyant weight) + 917.8

915 ppm-v: Dry weight (mg) = 1606.7 (Buoyant weight) + 528.0

Net calcification rates were normalized to coral fragment surface area (Table 3) and observational interval and expressed as mg (dry weight) cm^{-2} d^{-1}.

2.8 Photomicroscopic sample preparation

Representative numbers of coral specimens from all replicates of the four treatments were chosen to be cut and bleached in preparation for morphological analysis via photomicroscopy. Specimens with a minimum of ten suitable corallites were selected and sawed in half with an ethanol-cooled petrographic trim saw. Cut halves were then rinsed in ethanol and air dried.

Once dry, one half from each cut specimen was stored for subsequent analysis. The remaining half was then soaked for three hours in an 8.25% sodium hypochlorite solution to remove any organic residue that could obscure corallite morphology. Samples were given a final rinse with ethanol and air dried.

2.9 Measurement of corallite height

Corallite height (Table 4) was determined via stereomicroscopy (*Nikon SMZ1500*) as the difference in vertical position of the z-stage when the base versus the top of the corallite was in focus. Specimens from eleven equally represented colonies were selected from each of the four treatments in order to control for intercolonial variation. Corallites with predominantly flat surfaces were selected to ensure that vertical distances between the base and top of the corallite approximated true corallite height. A diminishing returns approach was used to determine that 3

corallites per specimen, 7 specimens per replicate, and 21 specimens per treatment were needed to obtain a normal distribution of data.

2.10 Measurement of septal infilling of the corallite

The percentage of septal infilling of the corallite was quantified via automated gray-scale image analysis of fully-focused top-down images of single corallites. Fully focused images of the corallites were obtained using a *Nikon SMZ1500* microscope fit with an automated z-stage system, a *Nikon Digital Sight DS-Ri1* camera, and *NIS Elements* image processing software. Images were captured using auto exposure (AE) and Auto White Balance (AWB) acquisition settings. Stage and room illumination were kept constant. The imaging software then aligned the focused portions of the separate images into a single fully focused image (Fig. 2a). This fully focused image was then imported into the image processing software program *ImageJ* and converted to an 8-bit grayscale photo (Fig. 2b). The contrast of this image was increased by 30% (Fig. 2c) to further separate positive space (i.e. septal infilling) from negative space (i.e., lack of septal infilling). The perimeter of the corallite of interest was manually cropped from the larger image (Fig. 2d), and the number of septa per corallite was manually counted and recorded. The histogram tool was then applied to the enhanced and cropped image to characterize the intensity of each pixel from 0 to 256, with 0 representing true black. A pixel intensity (PI) of 20 was selected as the divide between negative space ($PI \leq 20$; lack of septal infilling) and positive space ($PI > 20$; septal infilling), as $PI > 20$ was found to capture septal infilling within the corallite while excluding darker pigmentation resulting from the reflection of light off the base of the corallite (i.e., void space). The program *R* was employed to tally pixel intensity distribution, with percent septal infilling of a corallite calculated as the percentage of pixels with $PI > 20$, and then averaged by treatment.

2.11 Statistical analyses

Hierarchical linear mixed-effects models were utilized to fit this two-way factorial experiment with split-plot design to assess the additive and interactive effects of pCO_2 and temperature on the calcification rate, corallite height, and corallite infilling of *S. siderea* over the *ca.* 60-day experiment. Tanks represent plots, temperature and pCO_2 represent whole-plot treatments, and reef zones and coral colonies represent split-plot treatments. Random effects at the colony level were employed to account for variable coral specimen genotype, and random effects at the tank level were utilized to assess potential 'tank- effects' on the calcification response of each coral specimen. In this design, the random effects of tank and colony were therefore crossed and nested within the fixed effects of temperature, pCO_2, and reef zone. Five fixed effects models testing the additive and interactive effects of temperature, pCO_2, and reef zone were examined with the crossed random effects of tank and colony randomized at different levels of the model for a total of 20 models (Table 5).

All linear mixed-effects models were estimated using the *lme4* package of *R* 3.0.2 (Bates *et al.*, 2014). Restricted maximum likelihood (REML) was used to fit each model to calculate unbiased estimates of parameter variance and standard error. Akaike Information Criterion (AIC), which ranks models based on goodness of fit and parsimony, was used to identify the optimal combination of random effects (tank and colony) for the model-type that yielded the greatest number of significant predictors (Table 6) (Burnham and Anderson, 2002). Thus, optimal models (Table 7) were identified as the AIC-best fit model (i.e., lowest AIC score) that yielded the greatest number of significant predictors. Relative magnitude of the random effects is proportional to their reported variance (Table 7). The *AFEX*-package in R was used to obtain

parameter p-values (Tables 6,7) via the Kenwood-Roger approximation for degrees-of-freedom from the linear mixed-effects models (Singmann *et al.*, 2014).

3. EFFECT OF TEMPERATURE AND pCO_2 ON CALCIFICATION RATE

3.1 Results

3.1.1 Effect of temperature on calcification rate

Coral specimens under all temperature treatments continued to calcify on a net basis throughout the experiment, with calcification rates declining from the 28 °C to 32 °C treatments under both the normal and elevated pCO_2 conditions (Fig. 3a). In the low pCO_2 treatments, average calcification rates (±SE) decreased from 1.79 mg cm^{-2} d^{-1} (±0.16) to 0.71 mg cm^{-2} d^{-1} (±0.06) in the 28.1 °C (426 ppm-v) and 31.9 °C (424 ppm-v) treatments, respectively. In the high pCO_2 treatments, average calcification rates (±SE) decreased from 1.30 mg cm^{-2} d^{-1} (±0.10) to 0.27 mg cm^{-2} d^{-1} (±0.02) in the 28.0 °C (888 ppm-v) and 31.8 °C (940 ppm-v) treatments, respectively. Linear mixed effects modelling (Tables 5, 6) that controlled for the random effects of tank and colony revealed that temperature was a significant ($p = 0.0008$) predictor of calcification rate over the 60-day duration of the experiment (Table 7).

3.1.2 Effect of pCO_2 on calcification rate

Coral specimens under all pCO_2 treatments continued to calcify on a net basis throughout the experiment, with calcification rates declining from the control to the elevated pCO_2 treatments under both the 28 and 32 °C treatments (Fig. 3b). For the 28 °C treatments, average calcification rates (±SE) decreased from 1.79 mg cm^{-2} d^{-1} (±0.16) to 1.30 mg cm^{-2} d^{-1} (±0.10) in the 426 ppm-v (28.1 °C) and 888 ppm-v (28.0 °C) treatments, respectively. For the 32 °C treatments, average calcification rates decreased from 0.71 mg cm^{-2} d^{-1} (±0.06) to 0.27 mg cm^{-2} d^{-1} (±0.02) in the 424 ppm-v (31.9 °C) and 940 ppm-v (31.8 °C) treatments, respectively. Linear

mixed effects modelling (Tables 5, 6) that controlled for the random effects of tank and colony revealed that pCO_2 was a significant ($p = 0.04$) predictor of calcification rate over the 60-day duration of the experiment (Table 7).

3.1.3 Effect of reef zone on calcification response to temperature and pCO_2

Calcification rates of the experimental corals were evaluated from the three reef zones (nearshore, backreef, forereef) within each of the temperature-pCO_2 treatments (Fig. 4). The nearshore corals calcified faster than the forereef corals in the high pCO_2/28 °C treatment ($p < 0.008$; Fig. 4c). Those for the other reef zone/temperature/pCO_2 comparisons were not statistically significantly different ($p > 0.05$; Figs. 4a, b, d). Across all treatments, linear mixed effects modelling (Tables 5, 6) that controlled for the random effects of tank and colony revealed that reef zone was not a significant ($p > 0.05$) predictor of calcification rate over the 60-day duration of the experiment.

3.1.4 Effects of temperature and pCO_2 on bleaching

Coral bleaching, estimated here as a decrease in coral brightness and saturation (Siebeck *et al.*¸ 2006), was observed in the high temperature treatments (*ca.* 32 °C) at both 425 ppm-v and 915 ppm-v pCO_2 (Fig. 5). Sixty-four percent of corals reared at elevated temperature and normal pCO_2 exhibited some degree of bleaching, with 25% of specimens bleaching completely. Seventy-five percent of the specimens showed evidence of decreased brightness and saturation in the elevated temperature and elevated pCO_2 treatment, with 28% displaying a total loss of pigment. No bleaching was observed in corals exposed to average summertime temperatures (*ca.* 28 °C) for both the control and elevated pCO_2 treatments (Fig. 5).

Coral specimens reared in the high temperature treatments continued to calcify on a net basis throughout the experiment, with calcification rates declining from the non-bleached to the

bleached specimens under both the near-present-day and end of century pCO_2 treatments. Average calcification rates (±SE) decreased from 0.89 mg cm^{-2} d^{-1} (±0.13) to 0.60 mg cm^{-2} d^{-1} (±0.06) in the 424 ppm-v (31.9 °C) treatment and from 0.38 mg cm^{-2} d^{-1} (±0.06) to 0.23 mg cm^{-2} d^{-1} (±0.02) in the 940 ppm-v (31.8 °C) treatments (Fig. 6).

3.1.5 Model building

Linear mixed effects modelling (Tables 5, 6) that controlled for the random effects of tank and colony identified the temperature and pCO_2 model with random slopes for tank and colony (model 16; Table 7) to be the AIC-best fit model with the greatest number of significant predictors of calcification rate. The interactive effects of temperature and pCO_2 were not found to be significant, nor were the effects of reef-zone.

The following predictive equations were generated from the coefficients and intercepts of the best-fit linear mixed effects models identified in Table 7:

Calcification rate (0-60 d; mg cm^{-2} d^{-1}) = -0.27(±0.06) * T(°C) – 0.001(±0.0004) * pCO_2(ppm-v) + 9.73(±1.63)

3.2 Discussion

Coral calcification rates were significantly ($p < 0.05$) lower in the 32 °C treatments than in the 28 °C treatments for both the near-present-day and the high-pCO_2 treatments (Fig. 3a) and linear mixed effects modelling (Tables 5, 6) revealed that temperature is a significant ($p < 0.05$) negative predictor of calcification rate across all treatments (Table 7). These results show that the calcification rate of the coral *S. siderea* declines at temperatures predicted for the end of this century (*ca.* 32 °C) for the Belize portion of the MBRS (Castillo & Helmuth, 2005; Castillo & Lima, 2010; Castillo *et al.*, 2011; Castillo *et al.*, 2014). At this temperature, the zooxanthellae that reside symbiotically within the coral's tissues are expelled—a process known as bleaching

(Barnes and Hughes, 1999; Donner, 2009). Coral calcification is an energy intensive process (Cohen and McConnaughey, 2003; Ries, 2011) that requires energy provided by these symbiotic zooxanthellae in the form of translocated photosynthate. Thus, a decline in zooxanthellate abundance in the coral tissue should translate to a decline in available energy and thus a decline in calcification rate. Notably, coral bleaching resulted in significant ($p < 0.05$) decrease in average calcification rates within the high temperature treatments. Coral fragments reared at 32 °C under the near-present-day pCO_2 treatments that bleached experienced a thirty-two percent decline in average calcification rate as compared to those that did not (Fig. 6a). At high temperature and elevated pCO_2, the average calcification rate of bleached corals dropped by forty percent (Fig. 6b). The decline in coral calcification rate under the high-temperature conditions likely resulted from the bleaching that occurred under these conditions (Fig. 3a).

Coral calcification rates were also significantly lower ($p < 0.05$) in the high, predicted-end-of-century pCO_2 treatments, as compared to the near-present-day pCO_2 treatments, for both the 28 and 32° C treatments (Fig. 3b.) These results suggest that calcification within the scleractinian coral *S. siderea* will be impaired by CO_2-induced ocean acidification that is predicted for year 2100 (IPCC, 2007). These results are consistent with some studies investigating the impact of CO_2-induced ocean acidification on tropical corals (e.g., Langdon *et al.*, 2000; Crook *et al.*, 2013), but are not consistent with other studies on both tropical (e.g., Reynaud *et al.*, 2003; Jury *et al.*, 2009),temperate (e.g., Ries *et al.*, 2010; Holcomb *et al.*, 2010; Rodolfo-Metalpa *et al.*, 2010, 2011) and cold water (Maier *et al.*, 2011, 2013) scleractinian corals whose calcification rates were not impaired by comparable CO_2-induced ocean acidification. Collectively, these results support the assertion that the response of scleractinian

corals to ocean acidification is highly variable and complex (see Ries *et al.*, 2010, for detailed discussion).

Notably, the coefficient of the temperature effect on calcification (-0.270; Table 7) was substantially greater than the coefficient of the pCO_2 effect on calcification (-0.001), suggesting that the investigated change in temperature exerts a relatively stronger effect than the investigated change in pCO_2 on calcification rates of this coral species. This is supported by the observation that the linear mixed effect modelling identified temperature as a significant ($p < 0.05$) stand-alone predictor of calcification rate over the 0-60 day duration of the experiment, while pCO_2 was not identified as a significant stand-alone predictor of calcification rate (Table 6). Indeed, pCO_2 only became a significant predictor of calcification rate when it was combined with temperature in the additive model (Tables 6, 7). These results are consistent with a previous study (Castillo *et al.*, 2014) that showed that the isolated effects of predicted end-of-century warming on *S. siderea* calcification are more severe than the isolated effects of predicted end-of-century acidification.

However, the primary objective of the present study was to investigate the *combined* effects of ocean warming and acidification on tropical coral calcification, as these stressors should co-occur over the 21st century and beyond (IPCC, 2007b). Calcification rates for *S. siderea* between near-present-day pCO_2 (*ca.* 425 ppm-v) and predicted end-of-century pCO_2 (*ca.* 915 ppm-v; Fig. 7) declined by 27.5% at 28 °C and by 62.4% at 32 °C (Fig. 7). At near-present-day pCO_2 (*ca.* 425 ppm-v), calcification rates for *S. siderea* declined by 60.5% between 28 and 32 °C, while at predicted end-of-century levels (*ca.* 915 ppm-v), calcification rates declined by 79.5% with the same increase in temperature (Fig. 7). Thus, it was the elevated temperature/elevated pCO_2 treatment that yielded the slowest rate of coral calcification [0.27 mg

cm^{-2} d^{-1} (±0.02)] of the four treatments. Notably, this was also the only treatment to yield negative calcification rates (i.e., net dissolution) for some individual coral specimens, although the mean calcification rate for that treatment was positive (Table 3). Thus, although predicted end-of-century ocean warming appears to have a more deleterious impact on coral calcification rate than predicted end-of-century acidification (Castillo *et al.*, 2014), it is the combination of ocean warming and acidification that yields the worst outcome for calcification within this coral species. Nevertheless, the observation that the interactive effects of pCO_2 and temperature on calcification rate were not significant (Table 6) suggests that temperature and pCO_2 function additively, rather than synergistically (with synergistic effects defined as > additive effects), in their impact on the calcification rate of this species.

Castillo *et al.* (2012) used coral core data (*ca.* 1980-2010) to show that *S. siderea* from backreef and nearshore environments were not as negatively impacted by recent warming as *S. siderea* from forereef environments. They concluded from these observations that that exposure of backreef and nearshore colonies of *S. siderea* to historically greater baseline seasonal and diurnal thermal stress has increased their resistance/resilience to anthropogenic warming relative to forereef colonies, which have experienced more stable seawater temperatures throughout their evolutionary history. In the present experiment, calcification rates of *S. siderea* colonies were compared amongst reef zones to empirically evaluate Castillo *et al.*'s (2012) core-based observation that forereef colonies of *S. siderea* have been more vulnerable to warming than backreef and forereef colonies over the interval 1980-2010. Although forereef corals did exhibit lower average rates of calcification than those of backreef and nearshore corals in each of the treatments (Fig. 4a-d), it was only in the high-pCO_2/low-temperature treatment that calcification rates of forereef colonies were significantly ($p < 0.05$) lower than those of nearshore colonies

(Fig. 4c). Across treatments, linear mixed effects modelling revealed that reef zone was not a significant predictor of calcification rate (Table 6).

This is consistent with the observations, as the *ca.* 32 °C-915 ppm-v environment was the only treatment to yield negative calcification rates (i.e., net dissolution) for some individual specimens, although the mean calcification rate for that treatment was positive (Table 3).

4. EFFECT OF EXPERIMENTAL DURATION ON CALCIFICATION RESPONSE TO TEMPERATURE AND pCO_2

4.1 Results

4.1.1 Effect of exposure duration

Calcification rates were also evaluated over 0-30 and 30-60 day intervals (Fig. 8) to assess the impact of duration of exposure to elevated temperature and pCO_2 on coral calcification rate. For the *ca.* 28 °C treatments, calcification rates increased between the 0-30 d and 30-60 d observational intervals at 426 ppm-v, but remained largely unchanged between the 0-30 d and 30-60 d observational intervals at 888 ppm-v (Fig. 8a). For the *ca.* 32°C treatments, calcification rates decreased between the 0-30 d and 30-60 d observational intervals under both the low and high pCO_2 treatments (Fig. 8b). Linear mixed effects modelling (Tables 5, 6) that controlled for the random effects of tank and colony revealed that temperature ($p = 0.001$), but not pCO_2, was a significant predictor of calcification rate over the 0-30 d observational interval, while both temperature ($p = 0.001$) and pCO_2 ($p = 0.03$) were significant predictors of calcification rate over the 30-60 d observational interval (Table 7).

4.1.2 Model building

Linear mixed effects modelling that controlled for the random effects of tank and colony identified the temperature-only model (model 12; Table 6) and the temperature and pCO_2 model (model 16; Table 6), both with random slopes for tank and colony (Table 5), to be the AIC-best fit models with the greatest number of significant predictors of calcification rate for the 0-30 d and 30-60 d observational intervals, respectively (Table 7). The interactive effects of

temperature and pCO_2 were not found to be significant for either observational interval, nor were the effects of reef-zone.

The following predictive equations were generated from the coefficients and intercepts of the best-fit linear mixed effects models of calcification rates for the 0-30 day and 30-60 day observational intervals presented in Table 7:

Calcification rate (0-30 day; mg cm^{-2} d^{-1}) = -0.189(±0.043) * T(C°) + 6.624(±1.282)

Calcification rate (30-60 day; mg cm^{-2} d^{-1}) = -0.359(±0.080) * T(C°) – 0.002 (±0.001) * pCO_2(ppm-v) + 12.848(±2.400)

4.2 Discussion

Buoyant weights obtained at thirty-day intervals throughout the experiment revealed that for the *ca.* 28 °C treatments, the deleterious effect of increased pCO_2 on calcification rate was not observed until the second observational interval (30-60 d), with corals reared at near-present-day carbon dioxide levels calcifying at the rate of 2.27 ±0.21 mg cm^{-2} d^{-1} versus the rate of 1.24 ±0.11 mg cm^{-2} d^{-1} under the high pCO_2 treatment. This delayed response may result from progressive depletion of the coral's energy (lipid) reserves (e.g., Anthony *et al.*, 2007, 2009; Cohen and Holcomb, 2009; Castillo *et al.*, 2014), culminating during the second observational interval of the experiment.

The process of coral skeletal formation requires the removal of protons from a coral's calcifying fluid, which requires energy (Cohen and McConnaughey, 2003; Cohen and Holcomb, 2009; Ries, 2011). Removing protons from a calcifying fluid that is surrounded by seawater of higher proton concentrations (i.e., lower pH or 'more acidic') requires transporting protons across a stronger proton gradient, thereby requiring more energy (Ries, 2011). It is therefore possible that the reason the deleterious impacts of CO_2-induced ocean acidification on

calcification rates of *S. siderea* corals reared under the 28 °C are not observed until the 30-60 day observational interval is because it took more than 30-days for the coral's lipids energy reserves to become depleted by the increased energetic demands of transporting protons across a stronger proton gradient under the higher pCO_2-conditions.

In contrast, the reason that the deleterious effects of elevated pCO_2 on calcification were observed in both the first and second observational intervals of the high temperature treatments (ca. 32 °C treatments) may be because the combined stress of warming and acidification caused the corals' lipid energy reserves to become depleted in fewer than 30 days (i.e., during the first observational interval), with further declines observed during the second observational interval (Fig. 8b). Specifically, the depletion of energy reserves may have been accelerated by the combination of producing less photosynthate and/or lipid (due to thermally induced bleaching) and consuming photosynthate and/or lipids at a faster rate (due to enhanced proton-pumping under more acidic conditions).

This depletion of coral lipid reserves via ocean acidification was previously investigated by Schoepf *et al*. (2013). Four different species of tropical coral were reared in two temperatures and three pCO_2 levels for thirty days. They found mixed calcification rate responses among species to increased pCO_2, but determined that lipid reserves were largely unaffected. The study concluded that coral energy reserves were not used to maintain calcification levels in response to increased levels of carbon dioxide. This study, however, was only run for 30 days at a maximum temperature of 29 °C. Results of the present study on *S. siderea* suggest that this observational interval and temperature may not be sufficient to observe a material depletion in coral lipid reserves. The study findings also reveal that over short intervals (< 30 d), CO_2-induced ocean acidification (from ca. 425 to 915 ppm-v pCO_2) at 28 °C does not significantly impact the

calcification rate of the coral *S. siderea* (Fig. 8a; Table 7). This is consistent with the conceptual framework that corals possess the ability to maintain calcification rates in the short term by manipulating the carbonate chemistry of their calcifying medium (e.g., Ries *et al.*, 2009; Kreif *et al.*, 2010; Ries, 2010, 2011; Trotter *et al.*, 2011; Anagnostou *et al.*, 2012; McCulloch *et al.*, 2012; Venn *et al.*, 2012; Castillo *et al.*, 2014). Over longer intervals (i.e., > 30 d), it appears that ability of *S. siderea* to continue manipulating the carbonate chemistry of their calcifying medium is cumulatively impaired, such as through the progressive depletion of the corals' lipid energy reserves as discussed above.

The delayed effects of seawater warming and acidification on coral calcification rate may explain some of the variation in magnitude, and even direction, of calcification responses to warming and acidification observed in prior experiments on tropical corals that were conducted over varying durations (e.g., Marubini *et al.*, 2001, 2003; Comeau *et al.*, 2003; Langdon and Atkinson, 2005; Kleypas *et al.*, 2006; Schneider and Erez, 2006; Doney *et al.*, 2009; Krief *et al.*, 2010). Had the present experiment on *S. siderea* terminated at thirty days, no change in calcification rate would have been observed at 28 °C between low and high pCO_2. The experiment required an additional thirty days of observation for the accumulated stress of acidification to impact the corals' rate of calcification. Likewise, had the experiment been extended beyond 60 days, the negative response to CO_2-induced acidification may have become more severe or, should the corals acclimatize, become less severe. These results underscore the importance of conducting experiments investigating the effects of environmental stressors on coral calcification over various timescales, in order to assess short-, intermediate-, and long-term responses. Like for the 0-60 day observational interval, it was the combination of warming and acidification that yielded the most deleterious effects on calcification over both the 0-30 day and

30-60 day observational intervals. And the observation that the deleterious effects of CO_2-induced ocean acidification on calcification rate were observed earlier in the high temperature treatments than in the low temperature treatments supports this assertion. However, the observation that the interactive effects of pCO_2 and temperature on calcification rate were not significant across either observational interval (Table 6) supports the assertion that temperature and pCO_2 function additively, rather than synergistically, in their impact on the calcification rate of this species.

5. EFFECT OF TEMPERATURE AND pCO_2 ON CORALLITE MORPHOLOGY

5.1 Results

5.1.1 Impact of temperature on corallite height

Corallite height is defined here as the distance between the base and top of a single corallite—the cavity onto which the individual coral polyp is anchored and retracts into when threatened. Corallite heights were not significantly different ($p > 0.05$) between the 28 °C and 32 °C treatments under both the control and elevated pCO_2 conditions (Fig. 9a). There was no significant difference in average corallite heights between the low and high temperature treatments under near-present-day pCO_2 (28.1 °C/426 ppm-v: 1386.14 ±41.94 μm; 31.9 °C/424 ppm-v: 1305.53 ±56.07 μm), nor between the low and high temperature treatments under elevated pCO_2 (28.0 °C/888 ppm-v: 1199.03 ±52.36 μm; 31.8 °C/940 ppm-v: 1158.21 ±31.22 μm). Linear mixed effects modelling (Tables 5, 6) that controlled for the random effects of tank and colony confirmed that temperature was not a significant predictor of corallite height over the duration of the experiment.

5.1.2 Impact of pCO_2 on corallite height

Average corallite heights significantly ($p < 0.05$) declined from the control to the elevated pCO_2 treatments under both the low and high temperature conditions (Fig. 9b). For the ca. 28 °C treatments, average corallite heights (±SE) decreased from 1386.14 ±41.94 μm to 1199.03 ±52.36 μm from the 426 ppm-v (28.1 °C) to the 888 ppm-v (28.0 °C) treatments. For the ca. 32 °C treatments, average corallite heights decreased from 1305.53 ±56.07 μm to 1158.21 ±31.22 μm from the 424 ppm-v (31.9 °C) to the 940 ppm-v (31.8 °C) treatments. Linear mixed

effects modelling (Tables 5, 6) that controlled for the random effects of tank and colony confirmed that pCO_2 was a significant ($p = 0.003$) predictor of corallite height over the duration of the experiment (Table 7).

5.1.3 Impact of temperature on corallite infilling

Corallite infilling, defined as the percent of the corallite occupied by septal skeleton in plan view. There was no significant difference in average corallite infilling between the low and high temperature treatments under near-present-day pCO_2 (28.1 °C/426 ppm-v: 91 ±1%; 31.9 °C/424 ppm-v: 92 ±1%), nor between the low and high temperature treatments under elevated pCO_2 (28.0 °C/888 ppm-v: 85 ±1%; 31.8 °C/940 ppm-v: 86 ±1%) (Fig. 10a). Linear mixed effects modelling (Tables 5, 6) that controlled for the random effects of tank and colony confirmed that temperature was not a significant predictor of corallite infilling over the duration of the experiment.

5.1.4 Impact of pCO_2 on corallite infilling

Average corallite infilling significantly ($p < 0.05$) declined from the control to the elevated pCO_2 treatments under both the low and high temperature treatments (Fig. 10b). For the 28 °C treatments, average corallite infilling (±SE) increased from 85 ±1% to 91 ±1% from the 888 ppm-v (28.0 °C) to the 426 ppm-v (28.1 °C) treatments. For the 32 °C treatments, average corallite infilling increased from 86 ±1% to 92 ±1% from the 940 ppm-v (31.8 °C) to the 424 ppm-v (31.9 °C) treatments. Linear mixed effects modelling (Tables 5, 6) that controlled for the random effects of tank and colony confirmed that pCO_2 was a significant ($p = 0.0003$) predictor of corallite height over the duration of the experiment (Table 7).

A septal count was performed on each corallite evaluated in the study to evaluate whether a change in corallite infilling was a result of variations in the number of septa present within

corallites amongst the various treatments. The average number of septa per corallite (±SE) was found to be 46 ±2, 46 ±2, 45 ±1, and 47 ±1 for the 28.1 °C/426 ppm-v, 31.9 °C/424 ppm-v, 28.0 °C/888 ppm-v, and 31.8 °C/940 ppm-v treatments, respectively. These results indicate that the observed variation in corallite infilling resulted from CO_2-induced changes in the thickness of the coral septae in plan view, rather than from CO_2-induced changes in the number of septae within each corallite.

5.1.5 Model building

Linear mixed effects modelling (Tables 5, 6) that controlled for the random effects of tank and colony identified the pCO_2-only model with random slopes for tank and colony (model 20; Table 6) as the AIC-best fit model with the greatest number of significant predictors for both corallite height and corallite infilling. The interactive effects of temperature and pCO_2 were not found to be significant predictors of either corallite height or corallite infilling, nor were the effects of reef-zone (Table 6).

The following predictive equations were generated from the coefficients and intercepts of the best-fit linear mixed effects models of corallite height and corallite infilling presented in Table 7:

Corallite height (µm) = -0.357(±0.090) * pCO_2(ppm-v) + 1511.045(±72.394)

%-Corallite infilling = -0.000119(±0.0000210) * pCO_2(ppm-v) + 0.965(±0.0161)

5.2 Discussion

The coral skeleton begins with a structure known as the basal plate. This plate forms the template upon which the corallite of a young polyp will be built. Layers of aragonite are precipitated by the coral polyp to form a cup or depression (calix) in which the polyp will live and retreat into when threatened. The corallite is comprised of the theca (wall) and dissepiments

(radial partitions). The dissepiments form the base of the corallite and give it stability. The interior of the corallite (i.e., the calix) is divided by vertical plates (septae) radiating from the center. The columnella is found at the center of the corallite and is composed of the intertwining ends of the individual septa. These septae form the uppermost structure an individual corallite (Cohen and McConnaughey, 2003; Fig. 11).

Corallite height and %-corallite infilling were significantly lower ($p < 0.05$) in the high pCO_2 treatments than in the near-present-day pCO_2 treatments for both the 28 and 32 °C treatments (Figs. 9b and 10b) The observed reductions in corallite height and infilling under elevated pCO_2 are consistent with the observed reductions in net calcification rate under elevated pCO_2 (Fig. 3b; Table 7) and may define the mechanism—at least in part—by which CO_2-induced ocean acidification impairs calcification within this coral species. Conversely, since temperature did not appear to impact corallite geometry, but was observed to negatively impact coral calcification rate, temperature may impair calcification rates within this coral species simply by reducing the rate of vertical progradation of the entire corallite structure.

The observed reduction in corallite infilling under elevated pCO_2 is also consistent with the results of an 8-day experiment conducted at 25 °C by Cohen *et al.* (2009) that found that the cross-sectional skeletal area of new recruits of the tropical scleractinian coral *Favia fragum* was 75% lower under reduced Ω_A relative to the control treatment.

As measurements of corallite height and infilling reflect vertical and lateral accretion, respectively, of the corallite's septae, it is possible that CO_2-induced changes in the arrangement and/or habit of septal aragonite of *S. siderea* is the mechanism responsible for the observed reductions in corallite height and infilling.

Aragonite crystal habit becomes progressively more acicular with increasing rates of precipitation (i.e., more deviant from equilibrium conditions). Conversely, the equant crystal habit of aragonite is associated with slow growth in abiotic systems under conditions close to equilibrium (Cohen and McConnaughey, 2003; Holcomb et al., 2009). Thus, a CO_2-induced decrease in Ω_A could alter the habit of aragonite crystals comprising the coral skeleton (Cohen and McConnaughey, 2003). Indeed, Cohen et al. (2009) observed that aragonite needles comprising the sclerodermites (i.e., the aragonitic spherulites that represent the next highest structural unit of the coral skeleton above that of individual aragonite needles) of new recruits of *F. fragum* became shorter, wider and less organized with decreasing seawater pH. This decrease in the aspect ratio of coral aragonite under lower pH (Cohen *et al.*, 2009) could explain the observed decrease in both corallite height and infilling within *S. siderea* corals reared under elevated pCO_2.

Although a trend towards lower corallite heights under the higher temperature treatments was noted (Fig. 9a), it was not significant ($p > 0.05$). Hierarchical mixed effects modelling confirmed that pCO_2 was the only significant predictor of both corallite height and infilling (Table 6).

The results of the present study suggest that atmospheric pCO_2 predicted for the end of this century will alter the corallite geometry of *S. siderea* by reducing corallite height and degree of corallite infilling (Fig. 12). CO_2-induced reductions in corallite height would reduce the volume of the calyx into which the coral polyp can retreat when threatened, thus increasing the polyp's vulnerability to predation. CO_2-induced reductions in corallite infilling would reduce the biomechanical strength of the coral's protective corallite, thereby impairing the corallite's ability

to withstand mechanical impact and/or abrasion from high-force events such as storms, tsunamis, boat groundings, and parrotfish grazing.

6. CONCLUSION

The present study investigated the independent and combined effects of pCO_2 and temperature on the calcification rate and corallite morphology (corallite height and infilling) of the tropical reef-building coral *S. siderea*. Hierarchical linear mixed effect modelling of the results allowed the independent, additive, and interactive fixed effects of pCO_2, temperature, and reef-zone to be evaluated as predictors of coral calcification rate, corallite height, and corallite infilling, while controlling for the random effects of tank and colony.

The experiments reveal that both ocean warming and acidification impair calcification rates in the scleractinian coral *S. siderea*. Corals reared under pCO_2 predicted for year 2100 exhibited a decrease in calcification rate compared to those raised at near-present-day pCO_2. Although the CO_2-induced reduction in calcification rate was substantial, a more severe decline in calcification rate was observed as temperature was increased from a near-present-day level to a temperature predicted for year 2100, suggesting that warming poses the more immediate threat for this species of tropical reef-building coral. Predictive equations produced by the mixed effects modelling show that for every one degree C rise in temperature, an approximately 270 ppm-v rise in atmospheric pCO_2 is required to produce an equivalent decline in coral calcification rate.

It was the combination of warming and acidification, however, that yielded the lowest rate of calcification and the sharpest decline in calcification rate between observational intervals. Nevertheless, the lack of significance for interactive effects of pCO_2 and temperature on

calcification rate indicates that temperature and pCO_2 function additively, rather than synergistically, in their impact on the calcification rate of this species.

The deleterious effects of temperature and pCO_2 (at the higher temperature) on calcification rates were observed in both the first (0-30 d) and second (30-60 d) observational intervals of the experiment, while the deleterious effect of pCO_2 at the lower temperature was not observed until the second observational interval. The delayed onset of the deleterious effects of ocean acidification is consistent with the assertion that calcification in more acidic seawater can result in the progressive depletion of corals' lipid energy reserves—thereby limiting their ability to manipulate carbonate chemistry at their site of calcification. It also underscores the importance of experiment duration in assessing the response of corals to ocean warming and acidification and may partly explain apparent disparities in the coral calcification responses to these stressors as reported in prior studies.

Although average calcification rates for forereef colonies were consistently lower than calcification rates for backreef and nearshore colonies, consistent with the core-based observations of Castillo *et al.* (2012), these cross-reef differences were only statistically significant in the high-pCO_2/low-temperature treatment. And across treatments, the mixed effects modelling revealed that reef zone was not a significant predictor of calcification rate, corallite height, or corallite infilling. Differences in the vulnerability of corals from different reef zones to warming and acidification should be investigated via longer-term experiments, as such differences are critical for informing the decisions and actions of coral reef managers, policy makers, and legislators seeking to minimize the impact that CO_2-induced stressors will have on coral reef ecosystems in the years ahead.

Although numerous studies have documented the negatives effects of warming and acidification on calcification rates of scleractinian corals, few have investigated the impacts of these stressors on the skeletal morphology of corals. The present study on *S. siderea* reveals that CO_2-induced ocean acidification, but not warming, reduces corallite height and corallite infilling of this species. These changes in corallite geometry are consistent with past observations that the aspect ratio of both biogenic and abiogenic aragonite crystals is reduced when precipitated from seawater of reduced Ω_A. These CO_2-induced changes in corallite geometry are also consistent with the observation of the present study that pCO_2 was a significant predictor of coral calcification rate. Indeed, such alteration of corallite geometry may define, at least in part, the very mechanism by which ocean acidification impairs calcification rates within this species of coral. Conversely, since temperature did not appear to impact corallite geometry, but was observed to negatively impact coral calcification rate, it appears that temperature impairs calcification rates within this species simply by reducing the vertical progradation rate of the entire corallite structure.

CO_2-induced reductions in corallite height and corallite infilling would reduce both the volume of the calyx into which the coral polyp can retreat when threatened and the biomechanical strength of the coral's protective corallite, thereby increasing the polyp's vulnerability to predation and impairing the corallite's ability to withstand mechanical impact and/or abrasion from high-force events such as storms, tsunamis, boat groundings, and parrotfish grazing.

Corallite height and corallite infilling offer a relatively easily measured and ecophysiologically relevant parameter for quantifying the impact of ocean warming and acidification on coral skeletal morphology. Future studies should explore other morphological

changes in the coral skeleton that accompany ocean warming and acidification. Such information, in combination with the results of the present study, should prove useful in predicting and, potentially, mitigating the impacts of future CO_2-induced warming and acidification on coral reefs worldwide.

FIGURES

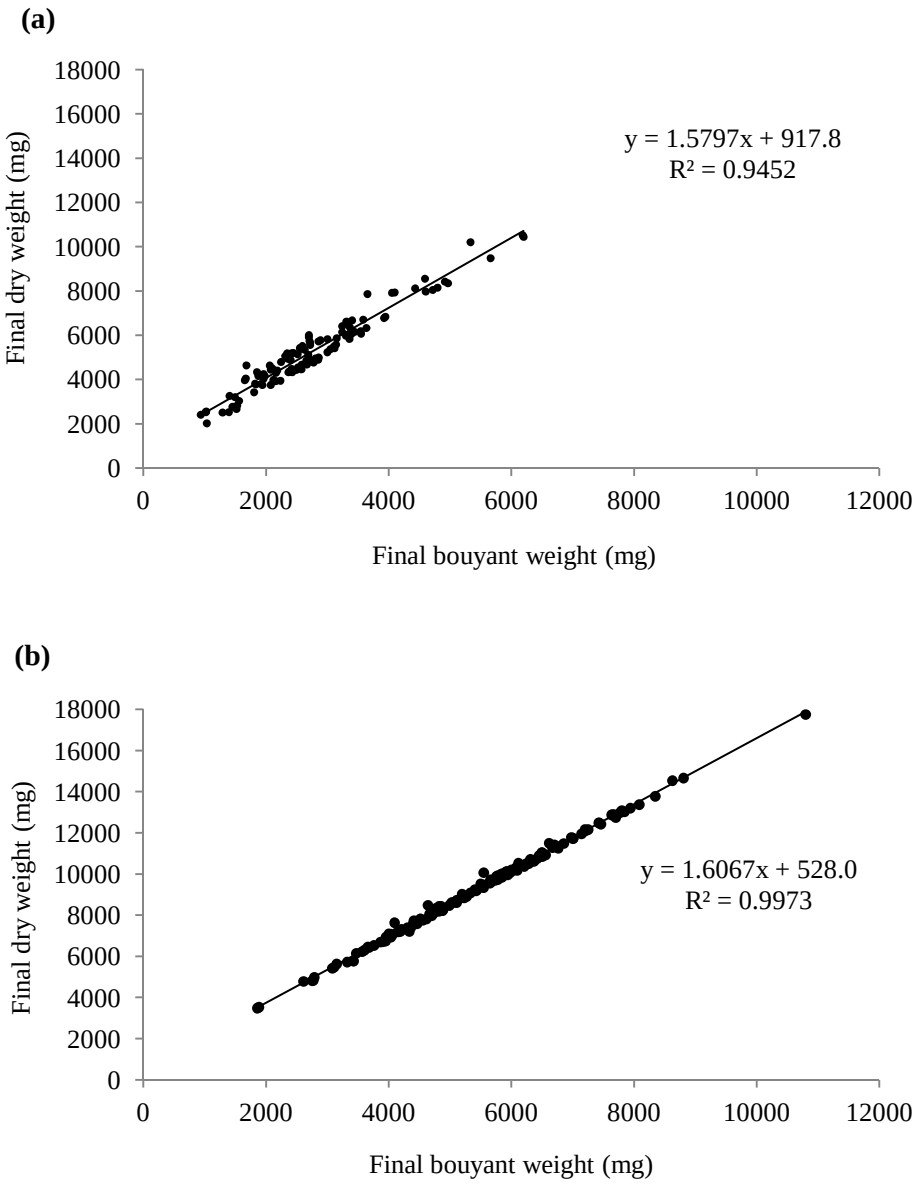

Figure 1. Plot of final buoyant weight vs. final dry weight for experimental *S. siderea* corals in low-pCO_2 (a) and high-pCO_2 (b) treatments. The strong linear correlation allows for estimation of initial dry weight from initial buoyant weight, for determination of net calcification rate.

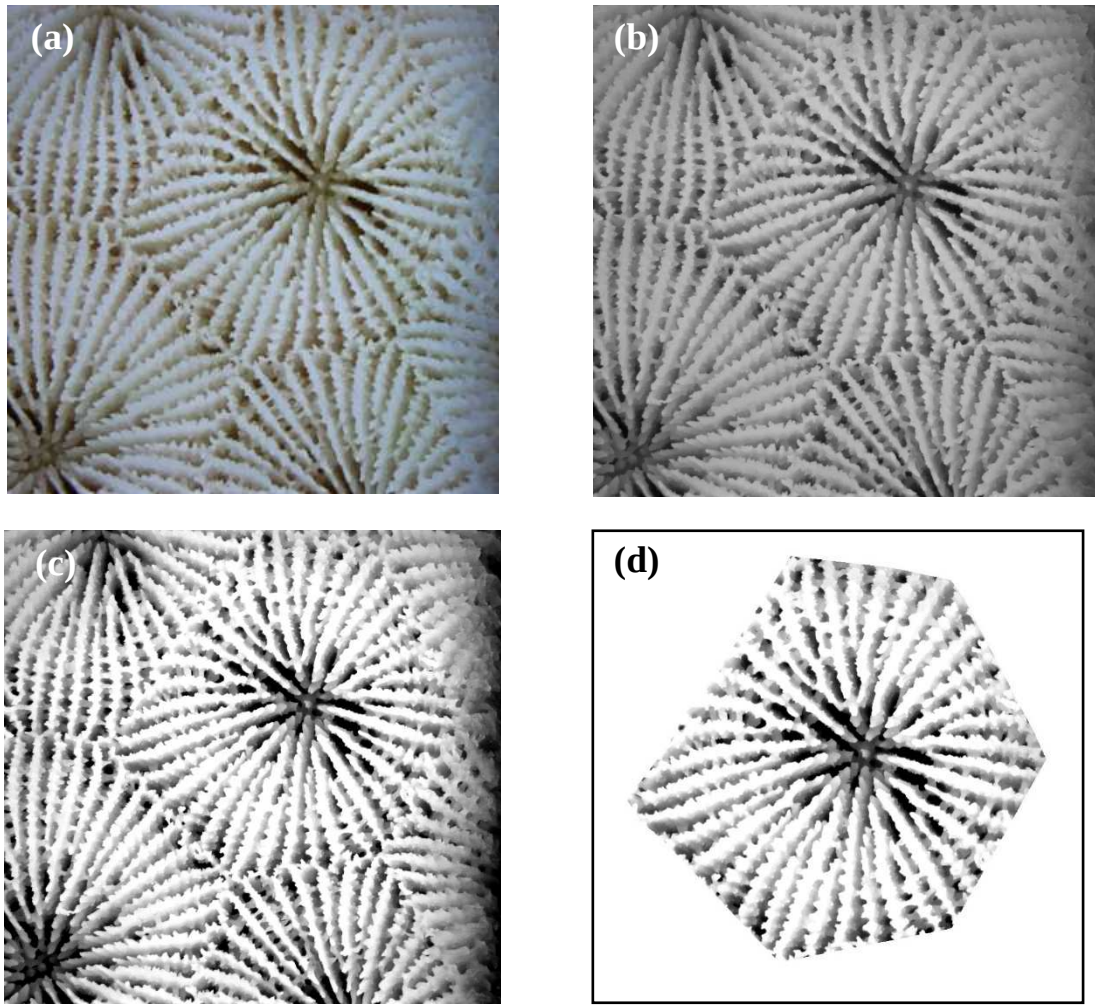

Figure 2. Progressive manipulation of *S. siderea* corallite photomicrographs for quantification of septal infilling. (a) Original aligned and focused micrograph. (b) 32-bit color image converted to 8-bit grayscale image. (c) Image contrast increased by 30%. (d) Cropped image of individual corallite.

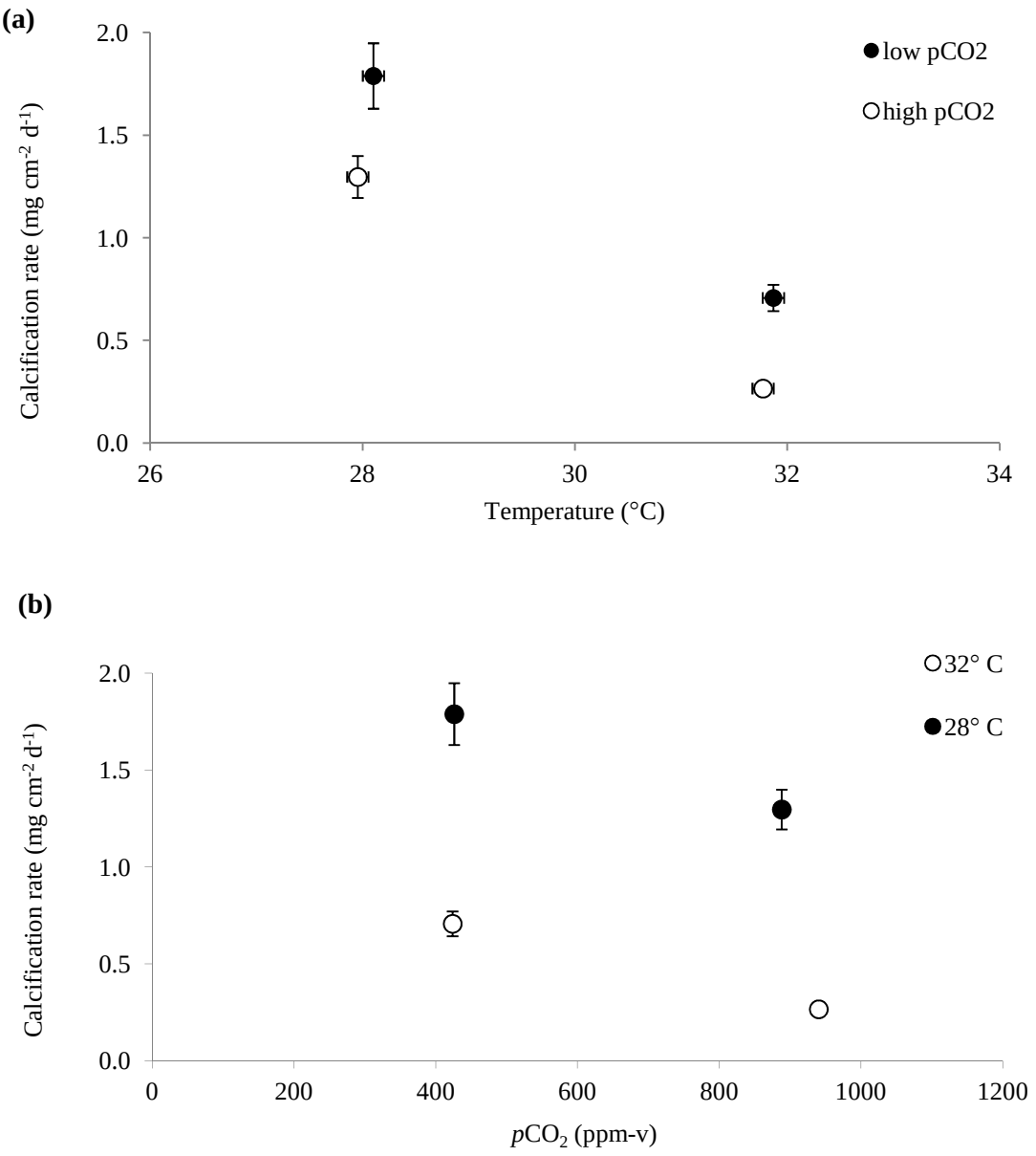

Figure 3. Average calcification rates for *S. siderea* corals reared at four crossed temperature-pCO_2 treatments (425 ppm-v-28 °C; 425 ppm-v-32 °C; 915 ppm-v-28 °C; 915 ppm-v-32 °C). (a) Temperature-effect for low and high-pCO_2 treatments. (b) pCO_2-effect for low and high-temperature treatments. Mixed effects modelling reveals that both pCO_2 and temperature are significant predictors of coral calcification rate across the duration of the sixty day experiment. Bars show standard error.

(a)

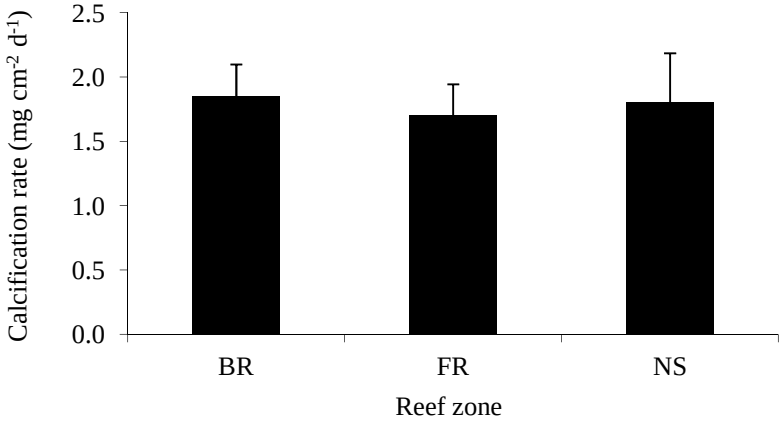
Calcification rate (mg cm-2 d-1)
2.5
2.0
1.5
1.0
0.5
0.0
BR
FR
NS
Reef zone

(b)

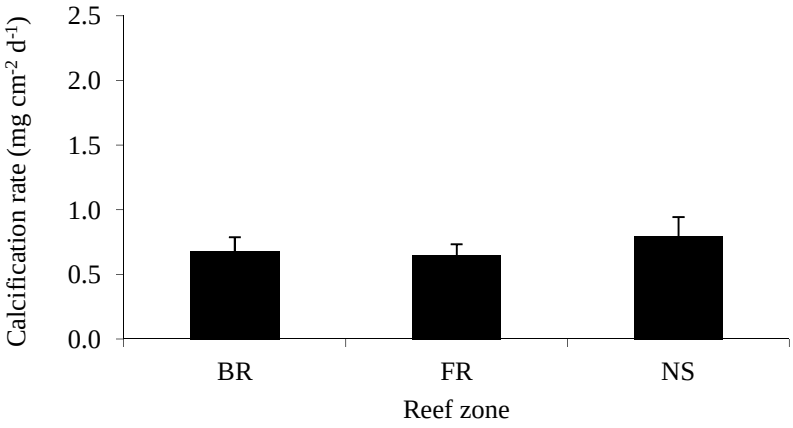
Calcification rate (mg cm-2 d-1)
2.5
2.0
1.5
1.0
0.5
0.0
BR
FR
NS
Reef zone

(c)

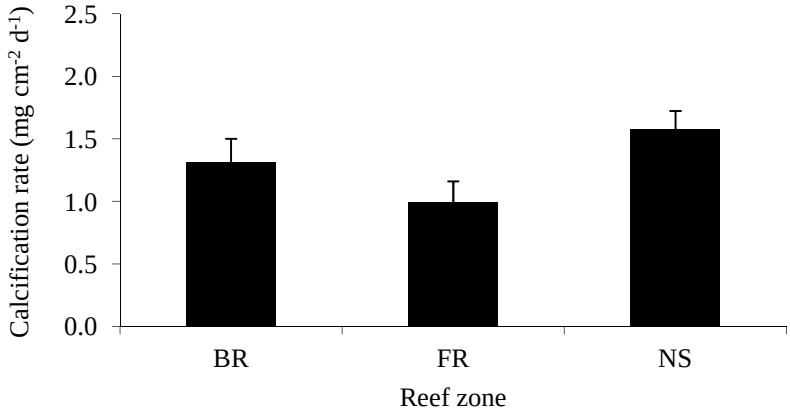
Calcification rate (mg cm-2 d-1)
2.5
2.0
1.5
1.0
0.5
0.0
BR
FR
NS
Reef zone

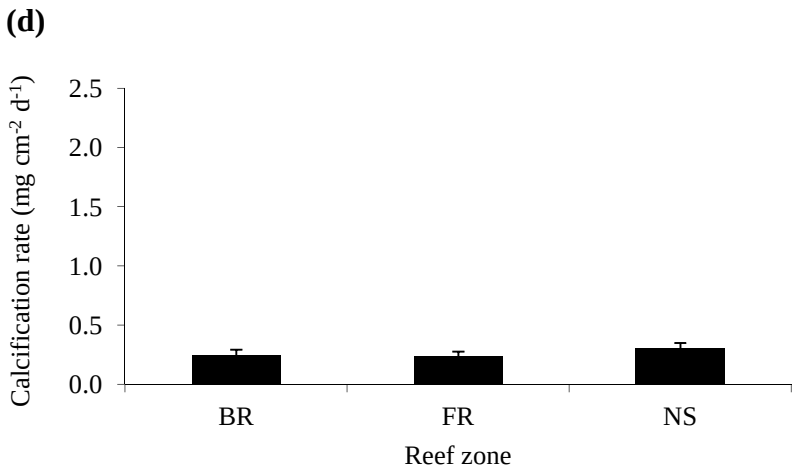

Figure 4. Calcification rates of *S. siderea* coral specimens from different reef zones ('BR' = backreef; 'FR' = forereef; 'NS' = nearshore) within the four temperature-pCO_2 treatments: (a) 425 ppm-v-28 °C; (b) 425 ppm-v-32 °C; (c) 915 ppm-v-28 °C; (d) 915 ppm-v-32 °C. No statistically significant differences in calcification rates amongst corals from the different reef zones were evident, with the exception that nearshore corals calcified significantly ($p < 0.05$) faster than forereef corals in the 915 ppm-v-28 °C treatment. Across treatments, mixed effects modelling reveals that reef zone was not a significant predictor of calcification rate or corallite geometry. Black vertical bars show standard error.

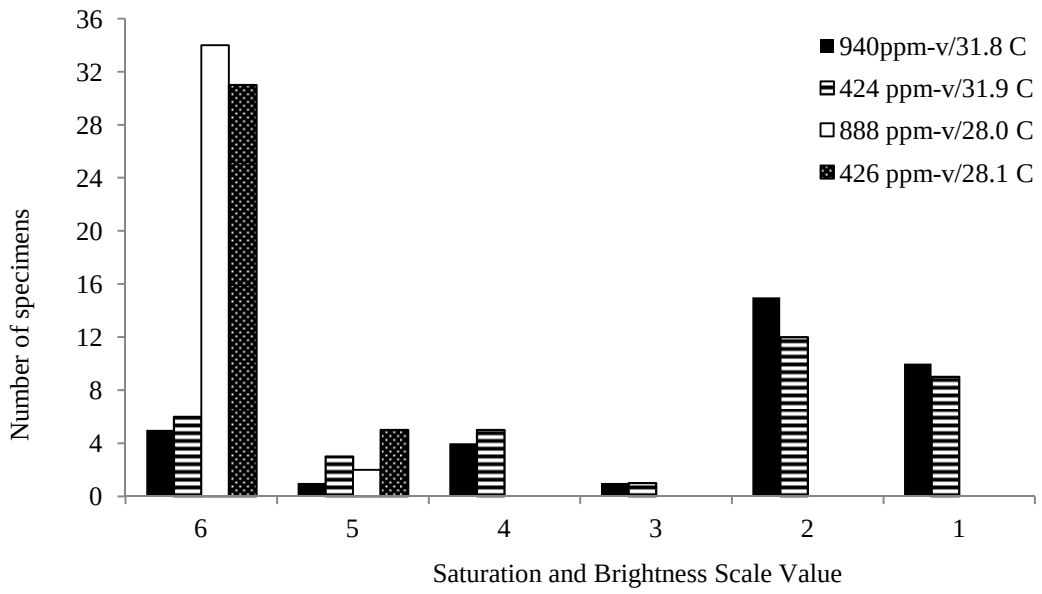

Figure 5. Histogram distribution of *Coral Watch Coral Health Chart* final saturation and brightness scale values (1 = no pigment; 6 = no loss of pigment) for the *S. siderea* specimens raised in the four temperature/pCO_2 treatments.

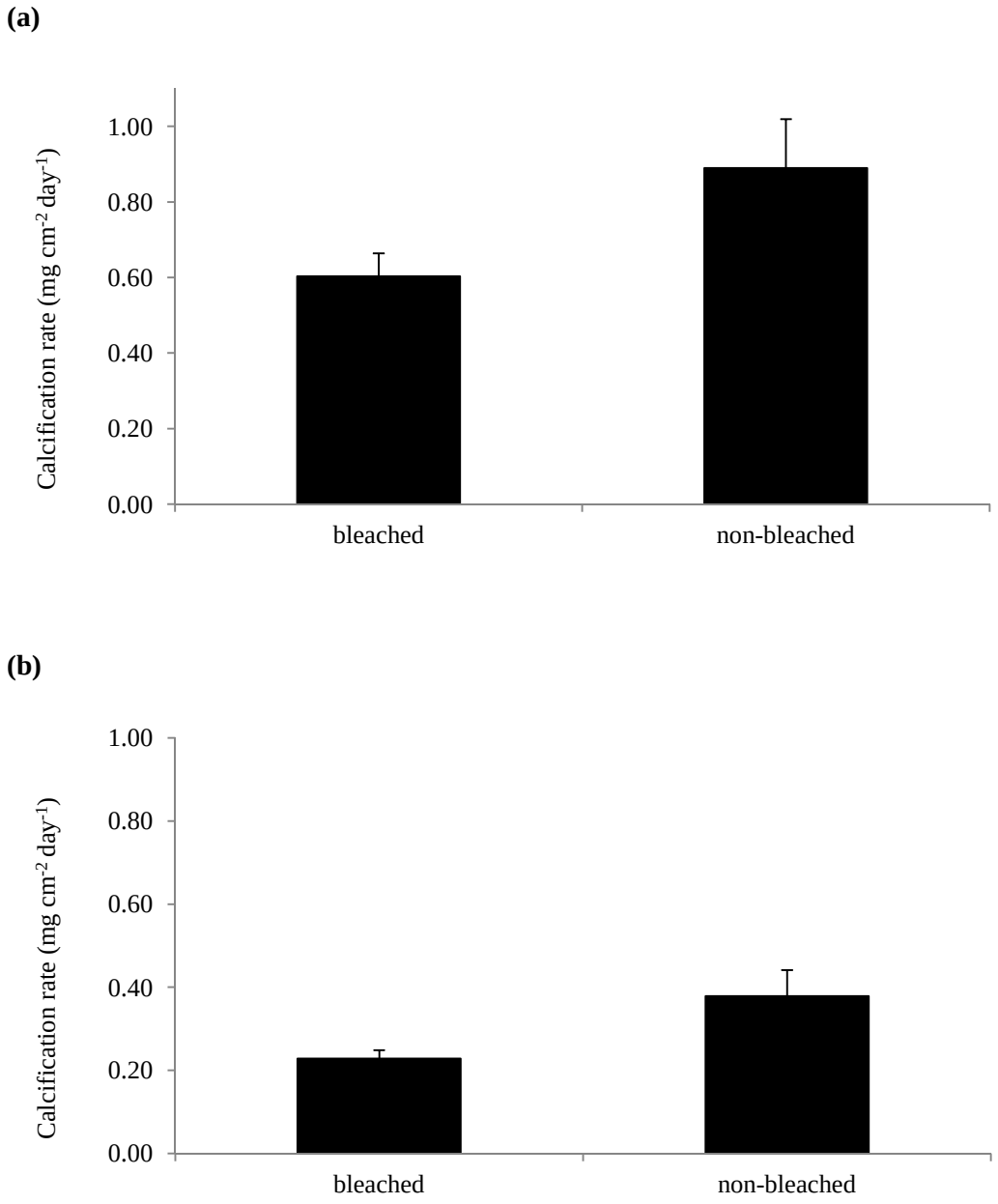

Figure 6. Average calcifications rate for bleached and non-bleached specimens of *S. siderea*: (a) 31.9 °C at 424 ppm-v (b) 31.8 °C at 940 ppm-v. Black vertical bars show standard error.

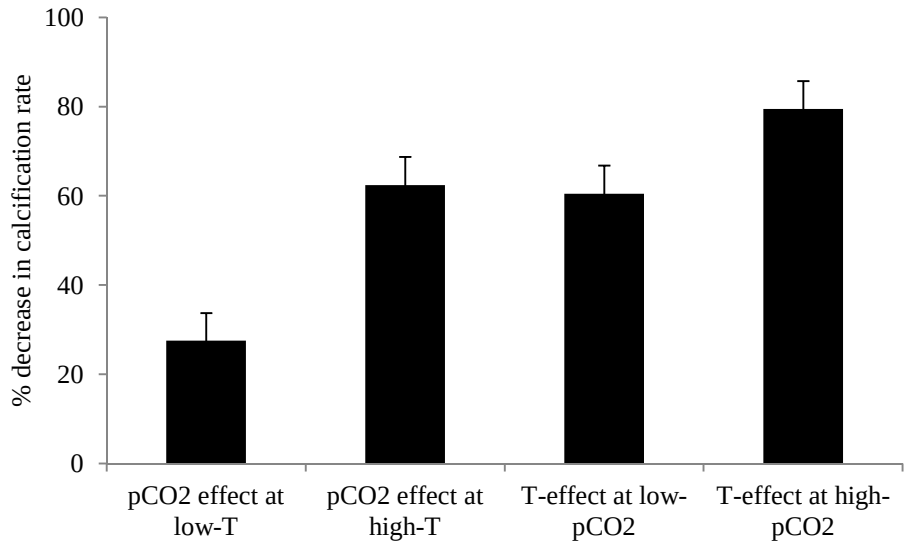

Figure 7. Percent-decrease in calcification rates amongst *S. siderea* coral reared in four crossed temperature-pCO_2 treatments: 888ppm-v/28.0 °C to 426 ppm-v/28.1 °C; 940 ppm-v/31.8 °C to 424 ppm-v/31.9 °C; 31.9 °C/424 ppm-v to 28.1 °C/426 ppm-v; 31.8 °C/940 ppm-v to 28.0 °C/888 ppm-v. Bars show standard error.

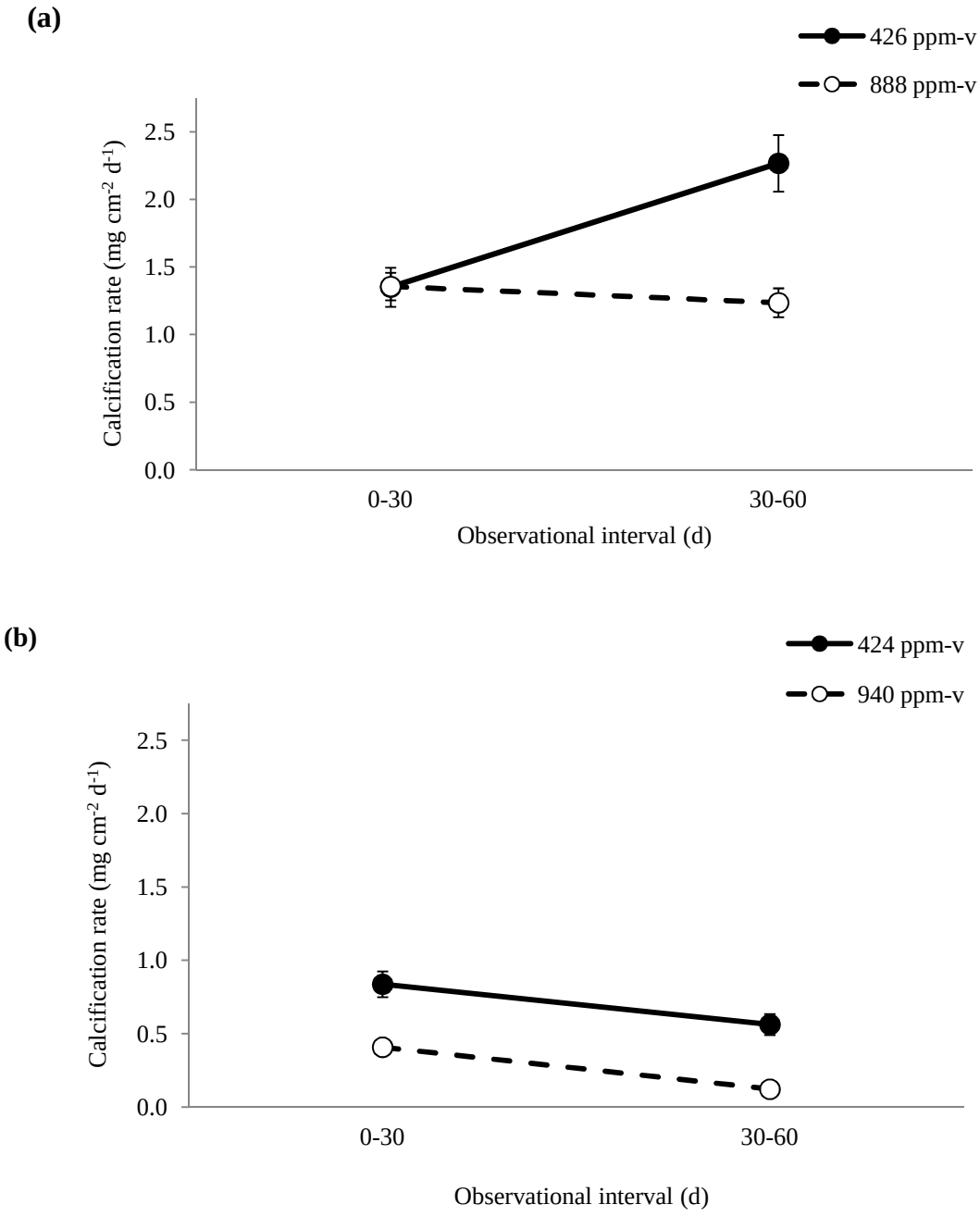

Figure 8. Average calcification rates for *S. siderea* corals reared under the control and elevated pCO_2 ppm-v conditions for the 0-30 and 30-60 day observational intervals at 28 °C (a) and 32 °C (b). Mixed effects modelling reveals that temperature only is a significant predictor of calcification rate across the 0-30 d observational interval, while both temperature and pCO_2 are significant predictors across the 30-60 d interval. Black vertical bars show standard error.

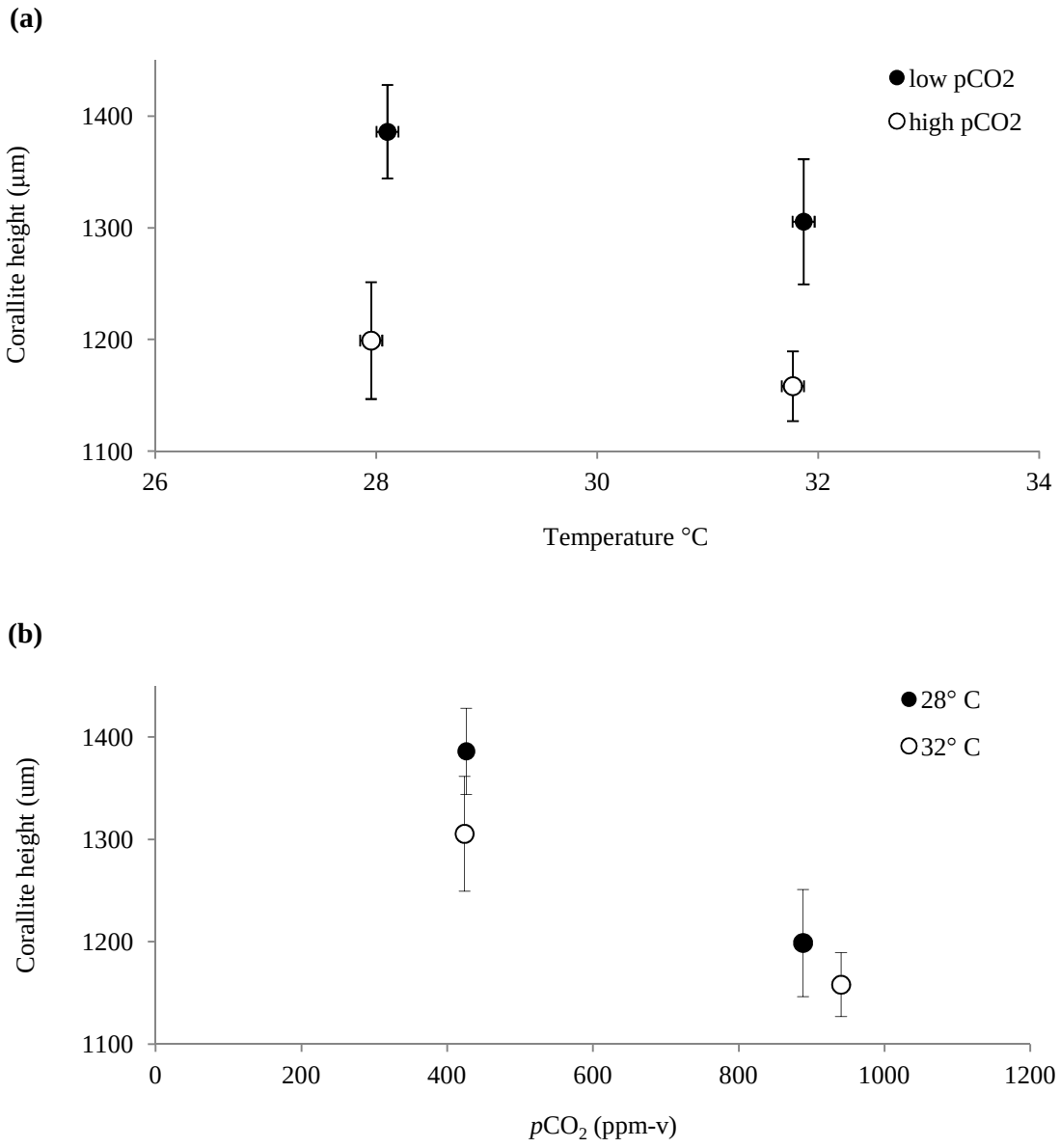

Figure 9. Average corallite heights for *S. siderea* corals reared at four crossed temperature-pCO_2 treatments: 28.1 °C/426 ppm-v; 28.0 °C/888 ppm-v; 31.9 °C/424 ppm-v; 31.8 °C/940 ppm-v. (a) Temperature-effect for low and high-pCO_2 treatments. (b) pCO_2-effect for low and high-temperature treatments. Mixed effects modelling reveals that pCO_2, but not temperature, is a significant predictor of corallite height. Bars show standard error.

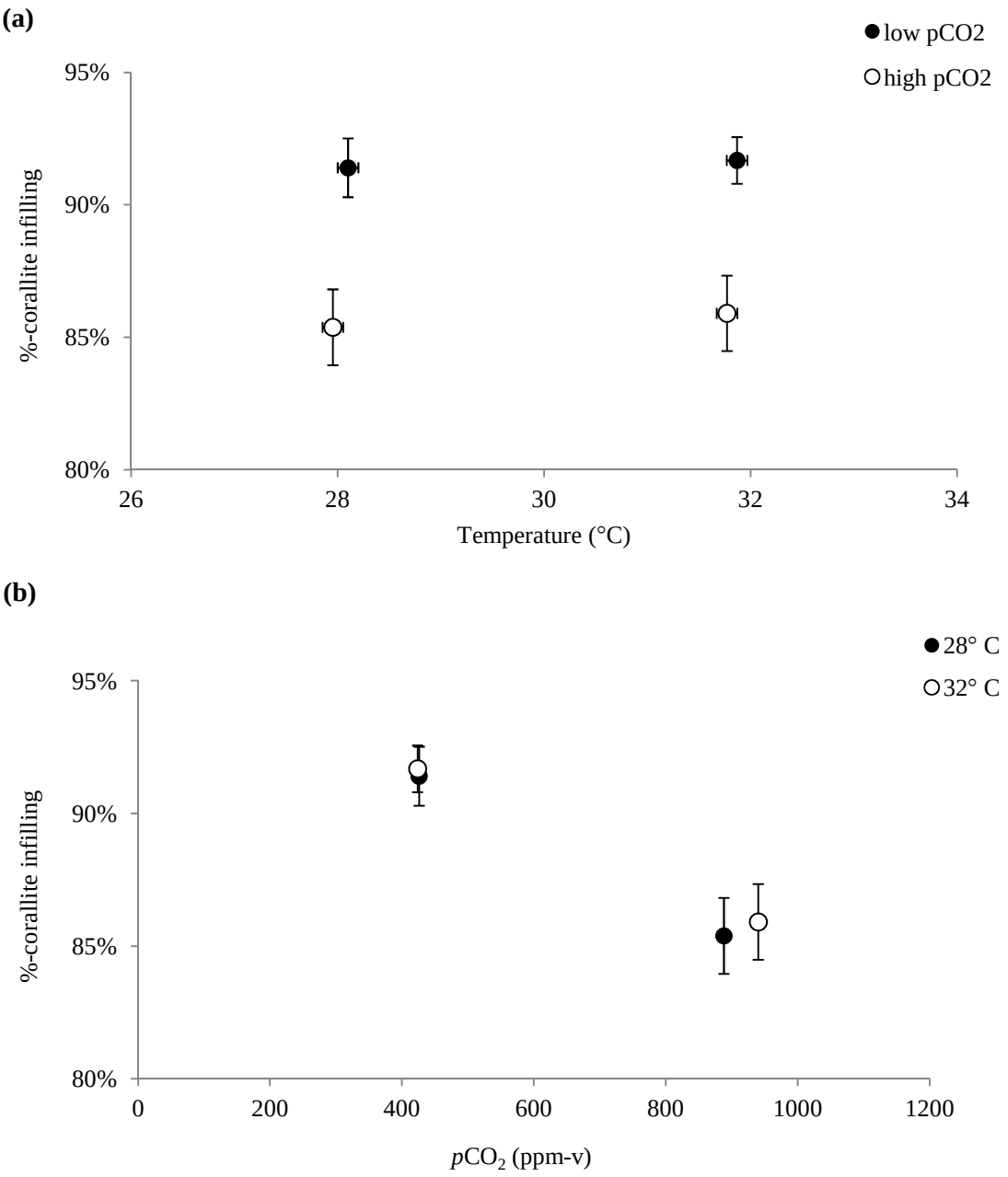

Figure 10. Percent-corallite infilling for *S. siderea* corals reared at four crossed temperature-pCO_2 treatments: 28.1 °C/426 ppm-v; 28.0 °C/888 ppm-v; 31.9 °C/424 ppm-v; 31.8 °C/940 ppm-v. (a) Temperature-effect for low and high-pCO_2 treatments. (b) pCO_2-effect for low and high-temperature treatments. Mixed effects modelling reveals that pCO_2, but not temperature, is a significant predictor of corallite height. Bars show standard error.

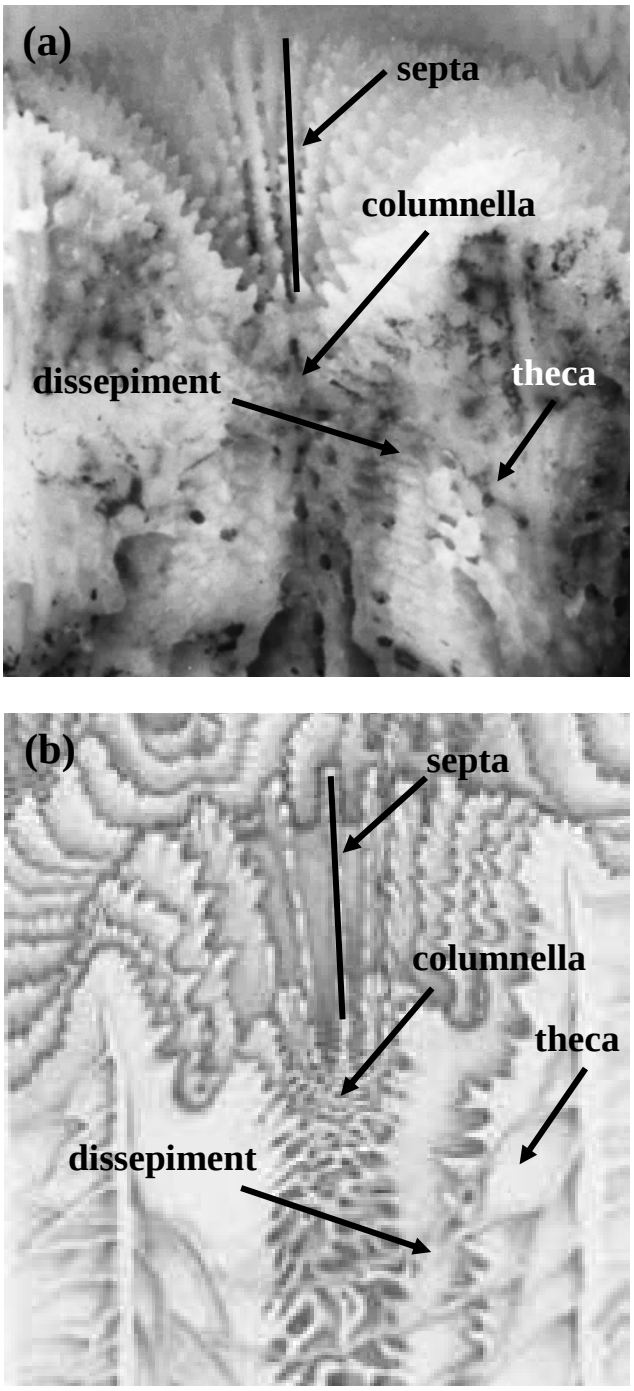

Figure 11. Cross-sectional photomicrograph (a; present study) and diagram (b; Veron, 1993) of the corallite structure showing septa, dissepiment, columnella, and theca. Black vertical bar shows corallite height as measured in the present study via stereomicroscopy.

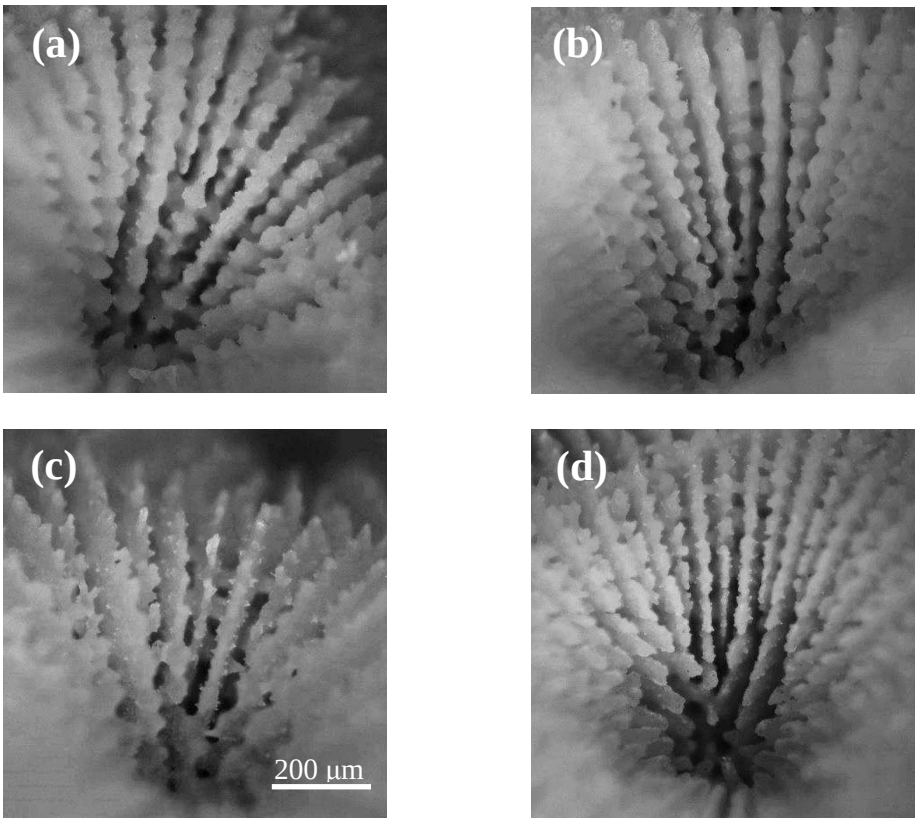

Figure 12. Photomicrographs of *Siderastrea siderea* specimens showing the combined effects of temperature and pCO_2 on corallite morphology. (a) 425 ppm-v at 28 °C. (b) 425 ppm-v at 32 °C. (c) 915 ppm-v at 28 °C. (d) 915 ppm-v at 32 °C.

TABLES

Table 1. Summary of recent studies investigating the effects of ocean acidification on scleractinian coral calcification.

Paper	Duration	Response	Water temperature
Hennige *et al.*, 2014	21 days	neutral	cold
Maier *et al.*, 2011	5 days	negative threshold	cold
Ries, Cohen, McCorkle, 2010	60 days	threshold negative	temperate
Holcomb *et al.*, 2010	6 months	negative	temperate
Rodolfo-Metalpa *et al.*, 2010	1 year	neutral	temperate
Ohki *et al*., 2013	6 weeks	negative	tropical
Movilla *et al.*, 2012	92 days	negative	tropical
Krief *et al.*, 2010	14 months	negative	tropical
Muehllehner & Edmunds, 2008	14 day	negative	tropical
Castillo *et al.*, 2014	90 days	parabolic	tropical

Table 2. Summary of average calculated and measured parameters for the temperature and pCO_2 treatments.

		425ppm/32 °C	425ppm/28 °C	915ppm/32 °C	915ppm/28 °C
CALCULATED PARAMETERS					
$\boldsymbol{pCO_{2\ (gas\text{-}e)}}$	(ppm-v)	424	426	940	888
	SE	10	11	10	14
	Range	349 - 537	334 - 522	824 - 1059	730 - 1018
	n	24	22	27	26
pH		8.09	8.10	7.80	7.77
	SE	0.01	0.01	0.01	0.01
	Range	7.93 - 8.16	7.96 - 8.19	7.76 - 7.85	7.69 - 7.85
	n	24	22	27	26
$\boldsymbol{[CO_3^{2-}]}$	(µM)	413	363	233	170

	SE	13	12	4	5
	Range	249 - 470	239 - 435	204 - 268	130 - 218
	n	24	22	27	26
$[HCO_3^-]$	(µM)	2069	2104	2338	2090
	SE	24	28	19	27
	Range	1797 - 2232	1873 - 2317	2240 - 2542	1857 - 2329
	n	24	22	27	26
$[CO_2]_{(SW)}$	(µM)	10.2	11.2	22.6	23.4
	SE	0.2	0.3	0.2	0.4
	Range	8 - 13	9 - 14	20 - 25	19 - 27
	n	24	22	27	26
Ω_A		6.8	5.8	3.8	2.7
	SE	0.2	0.2	0.1	0.1
	Range	4.1 - 7.7	3.8 - 7.0	3.4 - 4.4	2.1 - 3.5
	n	24	22	27	26
MEASURED PARAMETERS					
Sal		35.15	35.30	34.88	35.04
	SE	0.05	0.05	0.04	0.04
	Range	34.50 - 36.50	34.60 - 36.70	34.00 - 35.50	34.30 - 35.80
	n	81	81	78	78
Temp	(^{0}C)	31.9	28.1	31.8	28.0
	SE	0.1	0.1	0.1	0.1
	Range	31.0 - 32.7	27.5 - 29.1	31.1 - 32.1	27.7 - 28.3
	n	81	81	78	78
pH		8.14	8.08	7.89	7.82
	SE	0.01	0.01	0.01	0.01
	Range	8.00 - 8.28	8.01 - 8.18	7.75 - 8.21	7.62 - 8.18
	n	81	81	78	78
TA	(µM)	3024	2948	2878	2493
	SE	51	50	26	36
	Range	2404 - 3217	2459 - 3239	2723 - 3118	2190 - 2821
	n	24	22	27	26
DIC	(µM)	2492	2478	2593	2283
	SE	36	37	22	31
	Range	2065 - 2672	2133 - 2723	2470 - 2814	2017 - 2563
	n	24	22	27	26

Average calculated pCO_2 of the mixed gases in equilibrium with the experimental seawaters [pCO_2 (gas-e)], calculated pH, carbonate ion concentration [CO_3^{2-}], bicarbonate ion concentration [HCO_3^-], dissolved [CO_2] (SW), aragonite saturation state (Ω_A); and average measured salinity (Sal), temperature (Temp), measured pH, total alkalinity (TA), and dissolved inorganic carbon (DIC). “SE” is the standard error of the mean and “n” is the sample size.

Table 3. Dry weight, buoyant weight and surface area data for the coral specimens investigated in this experiment. Dry weights were calculated using the empirically derived buoyant weight-dry weight regression equations.

Treatment	Replicate	Colony	buoyant weight (mg)			dry weight (mg)			Surface area	Wt. normalized to surface area (mg cm^{-2})		
			0 d	**30 d**	**60 d**	**0 d**	**30 d**	**60 d**	**(cm^2)**	**0 d**	**30 d**	**60 d**
31.9 °C at	**1**	G	2359	2433	2493	4644	4761	4855	2.88	40.43	32.93	73.37
424 ppm-v		G	2940	2998	3047	5562	5654	5732	3.39	27.20	22.85	50.05
		H	1637	1669	1677	3504	3554	3567	1.88	26.59	7.00	33.59
		K	993	1012	1017	2486	2516	2525	1.37	21.46	6.52	27.98
		A	2003	2046	2100	4081	4149	4236	3.42	19.85	25.24	45.09
		A	3046	3100	3139	5729	5814	5876	4.18	20.41	14.74	35.15
		B	2316	2375	2398	4576	4670	4706	3.44	27.10	10.57	37.67
		C	1359	1383	1393	3065	3102	3119	2.64	14.17	6.39	20.56
		Q	2617	2651	2663	5052	5106	5124	2.99	18.12	5.98	24.10
		N	1570	1625	1651	3397	3484	3526	2.04	42.57	20.64	63.21
		O	3227	3292	3357	6016	6119	6221	3.77	27.26	27.12	54.38
		P	6088	6141	6184	10535	10619	10687	6.25	13.39	10.86	24.26
	2	G	2122	2194	2311	4269	4384	4569	3.14	36.45	59.12	95.57
		G	2853	2914	2997	5425	5522	5652	4.38	22.13	29.83	51.96
		H	1819	1821	1835	3791	3794	3817	2.01	1.57	11.26	12.83
		K	1819	1863	1953	3791	3861	4002	3.13	22.35	45.21	67.56
		A	3529	3578	3652	6493	6569	6687	3.60	21.23	32.80	54.03
		A	1577	1648	1668	3409	3521	3552	1.76	63.76	17.66	81.42
		B	2425	2544	2553	4748	4936	4951	3.01	62.52	5.08	67.59
		C	1749	1801	1818	3681	3763	3790	2.44	33.48	11.02	44.49
		P	4721	4745	4796	8376	8414	8494	4.90	7.74	16.23	23.97
		N	2458	2524	2592	4801	4905	5012	3.01	34.51	35.74	70.24
		O	2488	2636	2716	4848	5082	5208	2.99	78.39	42.28	120.68
		P	2808	2838	2856	5353	5401	5429	3.63	13.21	7.84	21.05

	3	G	2368	2397	2413	4658	4705	4730	2.38	19.69	10.62	30.31
		G	2021	2054	2074	4110	4163	4194	2.55	20.89	12.00	32.88
		H	3121	3132	3152	5848	5865	5898	3.20	5.43	10.21	15.64
		K	2129	2163	2181	4280	4335	4363	3.49	15.56	8.16	23.72
		A	4516	4555	4588	8052	8114	8166	5.30	11.71	9.83	21.54
		A	1780	1832	1849	3730	3812	3839	2.40	34.26	11.20	45.45
		A	2607	2667	2687	5036	5131	5162	5.61	17.07	5.53	22.60
		C	2509	2561	2575	4881	4964	4986	3.20	25.85	6.75	32.60
		M	3299	3393	3402	6129	6278	6292	2.69	55.48	5.29	60.77
		N	2204	2304	2342	4399	4557	4617	2.50	63.50	24.05	87.55
		O	3013	3055	3105	5677	5743	5823	4.51	14.70	17.62	32.33
		P	3970	4088	4095	7189	7376	7387	4.15	45.09	2.67	47.75
	28.1 °C at 426 ppm-v	**1**	G	1349	1430	1557	3049	3176	3377	2.29	55.37	87.76	143.13
			G	2095	2180	2364	4227	4361	4653	3.79	35.31	77.01	112.32
			H	2548	2612	2696	4943	5045	5176	2.37	42.88	55.55	98.43
			K	917	929	934	2366	2385	2393	1.50	12.67	4.93	17.60
			A	2870	3025	3240	5451	5696	6037	5.18	47.30	65.81	113.10
			A	2389	2442	2445	4692	4775	4780	2.17	38.38	2.43	40.80
			B	1754	1837	1954	3688	3819	4004	2.05	63.83	89.98	153.82
			C	2438	2571	2699	4769	4979	5181	2.48	84.72	81.32	166.04
			M	3353	3421	3549	6215	6322	6525	2.21	48.80	91.41	140.21
			N	2279	2503	2707	4517	4872	5195	3.03	117.17	106.39	223.56
			O	2554	2555	2580	4952	4954	4993	3.22	0.65	12.09	12.74
			P	4622	4628	4716	8220	8229	8368	4.25	2.10	32.68	34.78
		2	G	4216	4352	4602	7578	7792	8188	5.30	40.31	74.66	114.96
			G	1935	2044	2234	3975	4147	4446	2.70	63.60	111.01	174.61
			H	1837	1872	2157	3820	3876	4325	2.75	20.12	163.64	183.76
			K	1723	1872	2157	3639	3876	4325	2.80	84.50	160.72	245.22
			A	3275	3399	3544	6091	6287	6516	2.65	73.61	86.50	160.11
			A	1829	1939	2059	3807	3981	4170	2.73	63.75	69.34	133.09

			B	2150	2267	2415	4314	4500	4733	3.05	60.73	76.60	137.34
			C	1787	1921	2074	3741	3952	4194	2.40	88.13	100.40	188.53
			Q	870	948	1034	2292	2416	2551	1.24	99.71	108.62	208.34
			N	2146	2294	2551	4308	4541	4948	3.03	76.94	134.25	211.18
			O	3128	3233	3442	5859	6024	6355	3.84	43.07	86.00	129.07
			P	5449	5477	5659	9525	9570	9857	4.90	9.14	58.71	67.85
		3	G	2267	2321	2426	4499	4585	4751	2.90	29.59	57.18	86.76
			G	3853	3902	4052	7004	7082	7318	5.42	14.39	43.56	57.95
			H	2226	2278	2352	4434	4516	4633	2.80	29.51	41.55	71.06
			K	1243	1340	1492	2881	3034	3275	2.38	64.36	101.29	165.64
			A	1220	1237	1289	2845	2871	2954	1.83	14.39	45.18	59.56
			A	1728	1800	1872	3647	3761	3875	2.39	47.53	47.75	95.28
			F	2397	2444	2519	4704	4779	4898	3.74	20.01	31.85	51.87
			C	1414	1437	1450	3151	3188	3208	2.01	18.34	10.22	28.56
			M	2686	2732	2848	5161	5234	5417	3.48	20.87	52.63	73.50
			N	2351	2452	2586	4631	4791	5002	3.08	51.97	68.56	120.53
			O	2383	2513	2630	4682	4887	5072	3.02	68.05	61.24	129.29
			P	3866	3871	3945	7025	7033	7150	3.62	2.04	32.33	34.37
	31.8 °C at 940 ppm-v	**1**	A	5469	5518	5546	9315	9394	9439	5.30	14.86	8.49	23.35
			E	5058	5087	5104	8655	8702	8729	6.00	7.77	4.55	12.32
			D	2752	2769	2769	4950	4977	4976	4.55	6.00	-0.12	5.89
			E	3741	3770	3759	6538	6585	6568	5.10	9.23	-3.46	5.77
			G	6309	6354	6367	10664	10737	10758	7.09	10.28	2.95	13.22
			H	4782	4800	4814	8211	8240	8263	6.34	4.56	3.72	8.28
			K	4881	4886	4878	8370	8378	8365	4.70	1.71	-2.85	-1.14
			M	4383	4392	4396	7570	7585	7591	5.03	2.87	1.17	4.04
			P	5188	5216	5232	8864	8909	8934	6.44	6.98	3.91	10.89
			N	5161	5184	5194	8820	8857	8874	6.01	6.24	2.76	9.00
			P	6969	7008	7004	11726	11788	11781	6.37	9.75	-1.09	8.66
			R	5785	5824	5836	9823	9885	9905	7.02	8.78	2.90	11.68

	2	C	5051	5098	5093	8643	8719	8710	7.48	10.17	-1.22	8.95
		A	3257	3299	3321	5761	5829	5864	4.46	15.14	7.93	23.07
		E	5202	5264	5266	8887	8986	8989	5.67	17.58	0.57	18.15
		F	4311	4323	4319	7454	7473	7468	5.02	3.84	-1.07	2.78
		G	8632	8767	8805	14397	14613	14676	7.89	27.42	7.87	35.30
		I	3060	3100	3107	5445	5509	5519	4.33	14.85	2.48	17.33
		L	3879	3917	3948	6761	6821	6871	5.64	10.64	8.83	19.47
		M	6681	6761	6762	11263	11391	11393	5.47	23.48	0.20	23.68
		N	4803	4864	4874	8246	8344	8359	6.50	15.08	2.31	17.39
		O	4568	4632	4664	7867	7970	8022	5.01	20.44	10.38	30.82
		P	5764	5841	5859	9788	9913	9941	6.13	20.26	4.63	24.88
		P	6926	6999	7004	11656	11773	11781	6.42	18.18	1.25	19.43
	3	A	4079	4129	4159	7082	7162	7210	4.49	17.66	10.74	28.40
		D	5984	6047	6049	10142	10244	10247	6.88	14.79	0.47	15.26
		A	6515	6570	6613	10995	11083	11154	7.84	11.28	8.95	20.23
		F	4052	4092	4093	7038	7103	7105	4.56	14.21	0.47	14.67
		H	6042	6068	6093	10236	10277	10318	5.69	7.16	7.25	14.41
		I	6150	6202	6208	10409	10492	10503	6.48	12.82	1.65	14.47
		K	2689	2739	2752	4848	4929	4949	4.80	16.97	4.13	21.11
		L	4562	4591	4612	7858	7905	7938	5.20	8.96	6.38	15.34
		J	4633	4656	4697	7971	8008	8075	5.57	6.64	12.03	18.66
		O	5199	5299	5331	8881	9042	9093	6.25	25.79	8.22	34.01
		Q	7400	7440	7458	12417	12481	12511	8.06	7.97	3.72	11.69
		R	3575	3662	3681	6271	6412	6443	5.40	26.01	5.76	31.77
28.0 °C at 888 ppm-v	**1**	A	4959	5066	5199	8496	8668	8881	5.57	30.86	38.36	69.23
		C	3440	3523	3601	6055	6188	6314	5.09	26.10	24.84	50.94
		D	3390	3449	3470	5975	6069	6103	5.29	17.72	6.38	24.10
		E	5333	5589	5803	9096	9508	9852	6.37	64.74	53.89	118.63
		G	6884	7180	7424	11589	12065	12457	7.58	62.84	51.74	114.58
		H	5586	5652	5731	9502	9609	9737	5.80	18.38	21.98	40.37

	K	3668	3820	3928	6421	6666	6840	5.44	44.96	31.87	76.83
	L	5456	5649	5842	9294	9605	9914	5.78	53.73	53.55	107.28
	N	3080	3249	3426	5477	5749	6033	4.33	62.86	65.71	128.57
	O	4817	4974	5108	8267	8520	8736	4.90	51.68	43.92	95.60
	P	6087	6319	6557	10307	10681	11063	5.47	68.34	69.81	138.15
	Q	5304	5494	5672	9049	9355	9641	6.17	49.58	46.37	95.95
2	A	4457	4595	4729	7690	7911	8126	5.15	43.06	41.61	84.67
	B	4032	4173	4336	7006	7233	7494	3.82	59.54	68.22	127.76
	C	2962	3075	3150	5287	5469	5589	4.31	42.09	27.93	70.02
	F	4581	4693	4774	7888	8068	8198	5.76	31.25	22.51	53.75
	H	5886	5994	6100	9986	10159	10329	7.02	24.71	24.17	48.88
	I	6276	6389	6422	10612	10793	10846	7.01	25.82	7.49	33.31
	L	6266	6557	6853	10596	11063	11539	7.28	64.20	65.30	129.50
	M	3238	3457	3658	5730	6082	6405	5.28	66.55	61.28	127.83
	O	6097	6239	6447	10325	10553	10886	6.45	35.40	51.69	87.09
	N	6007	6390	6733	10179	10795	11345	7.55	81.46	72.88	154.35
	P	6821	7072	7251	11487	11890	12179	6.90	58.37	41.84	100.21
	R	4425	4626	4819	7638	7960	8270	7.36	43.76	42.16	85.92
3	D	2994	3029	3079	5339	5394	5474	4.73	11.67	16.99	28.66
	D	4140	4171	4186	7180	7229	7254	5.15	9.57	4.78	14.35
	E	5997	6106	6236	10163	10339	10547	5.87	29.92	35.49	65.41
	F	5764	5853	5914	9788	9931	10029	7.10	20.14	13.81	33.95
	G	5910	6196	6502	10023	10484	10975	6.98	65.96	70.41	136.37
	H	7825	7882	7938	13101	13191	13283	5.86	15.45	15.54	30.99
	K	4635	4770	4854	7976	8192	8326	5.83	37.20	22.96	60.16
	M	6338	6512	6670	10711	10990	11245	7.30	38.28	34.83	73.12
	N	3617	3823	4000	6339	6670	6955	5.93	55.94	47.99	103.93
	O	5501	5651	5778	9366	9607	9812	5.85	41.20	35.06	76.26
	Q	7253	7469	7631	12181	12528	12788	8.20	42.35	31.70	74.05
	R	4105	4162	4207	7124	7215	7287	5.02	18.15	14.41	32.56

Table 4. Corallite height measurements (μm) for selected *S. siderea* specimens investigated in this experiment.

Specimen	Replicate	Height (μm)	Specimen	Replicate	Height (μm)	Specimen	Replicate	Height (μm)	Specimen	Replicate	Height (μm)
		28.1 °C at 426 ppm-v			**31.9 °C at 424 ppm-v**			**28.0 °C at 888 ppm-v**			**31.8 °C at 940 ppm-v**
A104a	1	1670.3	A110a	1	1790.0	H7	1	1198.5	P12	1	1072.7
G4b		1409.0	A101a		1053.9	A17		1146.1	K5		1079.9
N102		1154.6	P101a		1419.6	K18		974.4	M13		886.1
P102a		970.6	O101a		1179.7	Q1		1778.5	A19		1298.6
A105a	2	1298.6	G19b		1209.4	P3		1315.8	P16		1335.3
P105a		1560.5	G1a		1072.5	G18		1203.5	G14		1429.5
G12a		1532.9	A102a	2	1068.2	O11		1169.0	H18		1138.0
KBb		1172.6	KBa		1172.4	M17	2	1483.8	N17		1000.9
O105a		1573.0	P105b		1252.3	F18		1279.2	P10	2	1057.3
P102b	3	1403.2	O104a		1147.9	H12		791.7	M3		1140.3
GS4a		1542.6	G4a		1317.0	A20		1086.7	P8		990.0
F16b		1408.7	HDa	3	1352.3	P17		1188.9	A109b		1500.6
N103b		1269.1	A103a		1236.3	N11		1034.8	O5		1183.2
OS7a		1547.9	P101b		1766.5	O20		1307.0	G15		1094.5
M109b		1262.9	O107a		1341.6	F15	3	1481.2	F4		1311.9
AS9a		1410.7	KCa		1509.1	M4		1216.8	A9	3	1094.1
HDb		1312.7				G8		1248.3	O18		1134.5
KCb		1450.8				H5		888.6	K13		1176.2
						K10		918.0	H11		1073.0
						N20		932.2	L7		1202.8
						Q13		1537.0	FS5		1223.8
									A15		1057.4

Table 5. Summary of the hierarchical linear mixed effects models evaluated in this study.

Model	Fixed Effects	Random Effects
1	Temperature*pCO_2*Reef Zone	Random Slopes and Intercepts for Tank and Colony
2	Temperature*pCO_2*Reef Zone	Random Slopes of Tank and Colony and Random Intercept for Colony
3	Temperature*pCO_2*Reef Zone	Random Slopes of Tank and Colony and Random Intercept for Tank
4	Temperature*pCO_2*Reef Zone	Random Slopes for Tank and Colony
5	Temperature*pCO_2	Random Slopes and Intercepts for Tank and Colony
6	Temperature*pCO_2	Random Slopes of Tank and Colony and Random Intercept for Colony
7	Temperature*pCO_2	Random Slopes of Tank and Colony and Random Intercept for Tank
8	Temperature*pCO_2	Random Slopes for Tank and Colony
9	Temperature	Random Slopes and Intercepts for Tank and Colony
10	Temperature	Random Slopes of Tank and Colony and Random Intercept for Colony
11	Temperature	Random Slopes of Tank and Colony and Random Intercept for Tank
12	Temperature	Random Slopes for Tank and Colony
13	Temperature+pCO_2	Random Slopes and Intercepts for Tank and Colony
14	Temperature+pCO_2	Random Slopes of Tank and Colony and Random Intercept for Colony
15	Temperature+pCO_2	Random Slopes of Tank and Colony and Random Intercept for Tank

16	Temperature+pCO_2	Random Slopes for Tank and Colony
17	pCO_2	Random Slopes and Intercepts for Tank and Colony
18	pCO_2	Random Slopes of Tank and Colony and Random Intercept for Colony
19	pCO_2	Random Slopes of Tank and Colony and Random Intercept for Tank
20	pCO_2	Random Slopes for Tank and Colony

Table 6. Summary of p-values and AIC output for each of the 20 hierarchical linear mixed effects models evaluated for 0-60 day calcification rate, 0-30 day calcification rate, 30-60 day calcification rate, corallite height, and corallite infilling. Model in bold contains the most significant ($p < 0.05$) fixed effects with random effects assigned by AIC (i.e., AIC-best-fit for model containing the most significant fixed effects).

0-60 day calcification	Model	Temperature	pCO_2	Temp:pCO_2	Reef Zone	Temp: Reef Zone	pCO_2: Reef Zone	Temp:pCO_2: Reef Zone	AIC
	1	0.09	0.65	0.75	0.51	0.52	0.35	0.38	378.46
	2	0.1	0.67	0.76	0.51	0.53	0.35	0.38	377.20
	3	0.08	0.65	0.75	0.50	0.52	0.34	0.37	377.90
	4	0.09	0.66	0.76	0.5	0.52	0.34	0.37	376.63
	5	0.08	0.63	0.72					289.85
	6	0.09	0.64	0.74					288.57
	7	0.08	0.62	0.72					289.62
	8	0.09	0.63	0.73					288.34
	9	0.001							261.95
	10	0.002							260.64
	11	0.001							261.78
	12	0.002							260.47
	13	0.0006	0.08						272.97
	14	0.0008	0.05						271.74
	15	0.006	0.08						272.75
	16	**0.0008**	**0.04**						**271.52**
	17		0.31						280.68
	18		0.22						278.87
	19		0.30						280.47
	20		0.21						278.65

0-30 day calcification	Model	Temperature	pCO_2	Temp:pCO_2	Reef Zone	Temp: Reef Zone	pCO_2: Reef Zone	Temp:pCO_2: Reef Zone	AIC
	1	0.69	0.3	0.26	0.27	0.31	0.15	0.18	388.21
	2	0.69	0.3	0.27	0.27	0.31	0.15	0.18	386.73
	3	0.68	0.3	0.27	0.26	0.29	0.14	0.17	387.61
	4	0.69	0.3	0.27	0.26	0.3	0.14	0.17	386.13
	5	0.67	0.29	0.25					302.50
	6	0.68	0.29	0.26					301.02
	7	0.67	0.29	0.26					302.62
	8	0.67	0.29	0.26					300.62
	9	0.001							271.99
	10	0.001							270.22
	11	0.001							271.59
	12	**0.001**							**269.83**
	13	0.001	0.29						286.42
	14	0.002	0.25						284.94
	15	0.001	0.29						285.99
	16	0.002	0.24						284.51
	17		0.5						291.77
	18		0.46						289.98
	19		0.49						291.32
	20		0.45						289.53

30-60 day calcification	Model	Temperature	pCO_2	Temp:pCO_2	Reef Zone	Temp: Reef Zone	pCO_2: Reef Zone	Temp:pCO_2: Reef Zone	AIC
	1	0.02	0.2	0.25	0.27	0.33	0.34	0.39	422.63
	2	0.03	0.22	0.27	0.27	0.33	0.34	0.4	421.40
	3	0.02	0.2	0.25	0.26	0.32	0.34	0.39	421.22
	4	0.03	0.21	0.27	0.26	0.32	0.34	0.39	419.99
	5	0.02	0.18	0.23					342.47

6	0.02	0.19	0.24					341.23
7	0.02	0.18	0.23					341.60
8	0.02	0.19	0.24					340.36
9	0.004							318.18
10	0.005							317.10
11	0.003							317.35
12	0.005							316.28
13	0.001	0.07						327.80
14	0.002	0.03						326.50
15	0.001	0.07						326.94
16	**0.001**	**0.03**						**325.64**
17		0.24						334.79
18		0.15						332.96
19		0.24						333.96
20		0.14						332.12

corallite height	Model	Temperature	pCO_2	Temp:pCO_2	Reef Zone	Temp: Reef Zone	pCO_2: Reef Zone	Temp:pCO_2: Reef Zone	AIC
	1	0.32	0.38	0.49	0.6	0.59	0.43	0.43	1028.43
	2	0.31	0.37	0.48	0.6	0.59	0.42	0.42	1026.43
	3	0.33	0.41	0.52	0.54	0.54	0.38	0.38	1026.92
	4	0.32	0.39	0.51	0.54	0.54	0.37	0.38	1024.92
	5	0.28	0.32	0.43					1038.25
	6	0.27	0.31	0.42					1036.25
	7	0.3	0.34	0.46					1037.04
	8	0.29	0.33	0.45					1035.04
	9	0.4							1038.05
	10	0.4							1036.08
	11	0.39							1036.75
	12	0.39							1034.76
	13	0.28	0.01						1032.67

14	0.28	0.004						1030.67
15	0.28	0.01						1031.40
16	0.28	0.005						1029.40
17		0.01						1038.82
18		0.003						1036.82
19		0.01						1037.52
20		**0.003**						**1035.52**

corallite infilling	**Model**	**Temperature**	***p*CO$_2$**	**Temp:*p*CO$_2$**	**Reef Zone**	**Temp: Reef Zone**	***p*CO$_2$: Reef Zone**	**Temp:*p*CO$_2$: Reef Zone**	**AIC**
	1	0.5	0.23	0.35	0.27	0.27	0.33	0.36	-2.16
	2	0.49	0.22	0.34	0.26	0.26	0.32	0.35	-4.16
	3	0.48	0.22	0.34	0.27	0.27	0.34	0.36	-4.15
	4	0.47	0.2	0.33	0.26	0.26	0.32	0.35	-6.15
	5	0.87	0.48	0.69					-121.89
	6	0.86	0.47	0.68					-123.89
	7	0.86	0.48	0.69					-123.89
	8	0.86	0.47	0.68					-125.89
	9	0.8							-147.19
	10	0.79							-149.08
	11	0.8							-149.19
	12	0.79							-151.08
	13	0.53	0.002						-144.66
	14	0.52	0.0006						-146.66
	15	0.52	0.002						-146.66
	16	0.51	0.0005						-148.66
	17		0.002						-156.17
	18		0.0004						-158.17
	19		0.001						-158.17
	20		**0.0003**						**-160.17**

Table 7. Summary of statistical parameters for hierarchical linear mixed effects model containing the most significant ($p < 0.05$) fixed effects with random effects assigned by AIC for 0-60 calcification rate (temperature and pCO_2), 0-30 day calcification rate (temperature only), 30-60 day calcification rate (temperature and pCO_2), corallite height (pCO_2 only), corallite infilling (pCO_2 only). Variance of random effects is proportional to the variability of the dependent variable (calcification rate, corallite height, corallite infilling) with respect to the random effect of interest (tank, colony).

0-60 day calcification	**Fixed effects**	**Value**	**SE**	***t*-value**	***p*-value**
	Intercept	9.73	1.63	5.99	
	Temperature	-0.270	0.06	-5.00	0.0008
	pCO_2	-0.000977	0.000420	-2.33	0.04
	Random effects	**Variance**	**SD**		
	Colony	0.0000490	0.00700		
	Tank	0.000116	0.0108		

0-30 day calcification	**Predictor**	**Value**	**SE**	***t*-value**	***p*-value**
	Intercept	6.62	1.28	5.17	
	Temperature	-0.19	0.04	-4.38	0.001
	Random effects	**Variance**	**SD**		
	Colony	0.0000658	0.00811		
	Tank	0.0000624	0.00790		

30-60 day calcification	Predictor	Value	SE	*t*-value	*p*-value
	Intercept	12.85	2.40	5.36	
	Temperature	-0.36	0.08	-4.51	0.001
	pCO_2	-0.002	0.001	-2.61	0.03
	Random effects	**Variance**	**SD**		
	Colony	0.0000414	0.00643		
	Tank	0.000269	0.0164		

Corallite height	Predictor	Value	SE	*t*-value	*p*-value
	Intercept	1511.05	72.39	20.87	
	pCO_2	-0.36	0.09	-3.97	0.003
	Random effects	**Variance**	**SD**		
	Colony	4.945	2.224		
	Tank	0.000	0.000		

Corallite infilling	Predictor	Value	SE	*t*-value	*p*-value
	Intercept	0.965	0.0161	60.06	
	pCO_2	-0.000119	0.0000210	-5.66	0.0003

Random effects	Variance	SD
Colony	0.000000136	0.000369
Tank	0.000	0.000

REFERENCES

Anagnostou E, Huang KF, You CF, Sikes EL, Sherrell RM (2012) Evaluation of boron isotope ratio as a pH proxy in the deep sea coral< i> Desmophyllum dianthus</i>: Evidence of physiological pH adjustment. *Earth and Planetary Science Letters*, **349**, 251-260.

Anthony KRN, Connolly SR, Hoegh-Guldberg O (2007) Bleaching, energetics and coral mortality risk: effects of temperature, light, and sediment regime. *Limnology & Oceanography*, **52**, 716 –726.

Anthony KRN, Hoogenboom MO, Maynard JA, Grottoli AG, Middlebrook R (2009) Energetics approach to predicting mortality risk from environmental stress: a case study of coral bleaching. *Functional Ecology*, **23**, 539-550.

Atkinson MJ, Bingman C (1998) Elemental composition of commercial seasalts. *Journal of Aquariculture and Aquatic Sciences*, **2**, 39-43.

Barnes R, Hughes R (1999) *An Introduction to Marine Ecology*, Blackwell Science, Inc., Malden, MA.

Burnham K, Anderson D (2002) *Model Selection and Multimodel Inference: A Practical Information-Theoretic Approach*, pp. 60-64, Springer Verlag, New York, NY, USA.

Caldeira K, Wickett ME (2003) Oceanography: Anthropogenic carbon and ocean pH. *Nature*, **425**, 365-365.

Cantin NE, Cohen AL, Karnauskas KB, Tarrant AM, McCorkle DC (2010) Ocean warming slows coral growth in the central red sea. *Science*, **329**, 322-325.

Carilli JE, Norris RD, Black BA, Walsh SM, McField M (2009) Local stressors reduce coral resilience to bleaching. *PLoS One*, **4**, e6324.

Castillo KD, Helmuth BST (2005) Influence of thermal history on the response of Montastraea annularis to short-term temperature exposure. *Marine Biology*, **148**, 261- 270.

Castillo KD, Lima FP (2010) Comparison of in situ and satellite-derived (MODIS Terra/Aqua) methods for assessing temperatures on coral reefs. *Limnology and Oceanography: Methods*, **8**, 107-117.

Castillo KD, Ries JB, Weiss JM (2011) Declining coral skeletal extension for forereef colonies of Siderastrea siderea on the Mesoamerican Barrier Reef System, southern Belize. *PLoS ONE*, **6**, e14615.

Castillo KD, Ries JB, Weiss JM, Lima FP (2012) Decline of forereef corals in response to recent warming linked to history of thermal exposure. *Nature Climate Change*, **2**, 756-760.

Castillo KD, Ries JB, Bruno JF, Westfield IT (2014) The reef-building coral *Siderastrea siderea* exhibits parabolic responses to ocean acidification and warming. Proceedings of the Royal Society of London B: Biological Sciences, **281**, 20141856, doi:10.1098/rspb.2014.1856.

Cohen AL, McConnaughey TA (2003) Geochemical perspectives on coral mineralization. *Reviews in Mineralogy and Geochemistry*, **54**, 151-187.

Cohen AL, Holcomb M (2009) Why corals care about ocean acidification: Uncovering the mechanism. *Oceanography*, **22**, 118–127.

Cohen AL, McCorkle DC, de Putron S, Gaetani GA, Rose KA (2009) Morphological and compositional changes in the skeletons of new coral recruits reared in acidified seawater: insights into the biomineralization response to ocean acidification. *Geochemistry Geophysics Geosystems*, **10**, Q07005, doi:10.1029/2009GC002411.

Coles SL, Jokiel PL (1977) Effects of temperature on photosynthesis and respiration in hermatypic corals. *Marine Biology*, **43**, 209-216, doi:10.1007/bf00402313.

Comeau S, Edmunds P, Spindel N, Carpenter R (2013) The response of eight coral reef calcifiers to increasing partial pressure of CO_2 do not exhibit a tipping point. *Limnology and Oceanography*, **58**, 388-398, doi:10.4319/lo.2013.58.1.0388.

Cooper TF, De'ath G, Fabricius KE, Lough JM (2007) Declining coral calcification in massive Porites in two nearshore regions of the northern Great Barrier Reef. *Global Change Biology*, **14**, 529–538.

Crook ED, Cohen AL, Rebolledo-Vieyra M, Hernandez L, Paytan A (2013) Reduced calcification and lack of acclimation by coral colonies growing in areas of persistent natural acidification. *PNAS*, **110**, 11044–11049, doi/10.1073/pnas.1301589110.

De'ath, G, Lough JM, Fabricius KE (2009) Declining coral calcification on the Great Barrier Reef. *Science*, **323**, 116-119.

Dodge RE, Lang JC (1983). Environmental correlates of hermatypic coral (Montastrea annularis) growth on the East Flower Gardens Bank, northwest Gulf of Mexico. *Limnology and Oceanography*, **28**, 228-240.

Doney SC, Fabry VJ, Feely RA, Kleypas JA (2009) Ocean acidification: The other CO_2 problem. *Annual Review of Marine Science*, **1**, 169–192.

Donner, SD (2009) Coping with commitment: Projected thermal stress on coral reefs under different future scenarios. *PLoS ONE* , **4**, 1-10.

Eakin CM, Kleypas J, Hoegh-Guldberg O (2008) Global climate change and coral reefs: rising temperatures, acidification and the need for resilient reefs. In: *Status of coral reefs of the*

world (ed. Wilkinson C), pp. 29–34. Global Coral Reef Monitoring Network and Reef and Rainforest Research Centre, Townsville, Australia.

Etheridge DM, Steele LP, Langenfelds RL, Francey RJ, Barnola JM, Morgan VI (2012) Natural and anthropogenic changes in atmospheric CO_2 over the last 1000 years from air in Antarctic ice and firn. *Journal of Geophysical Research*, **101**, 4115–4128.

Fabry VJ, Seibel BA, Feely RA, Orr JC (2008) Impacts of ocean acidification on marine fauna and ecosystem processes. *ICES Journal of Marine Science*, **65**, 414–432.

Gattuso JP, Frankignoulle M, Bourge I, Romaine S, Buddemeier RW (1998) Effect of calcium carbonate saturation of seawater on coral calcification. *Global Planet Change*, **18**, 37–46.

Gischler E, Oschmann W (2005), Historical climate variation in Belize (Central America) as recorded in scleractinian coral skeletons. *Palaios*, **20**, 159-174.

Glynn PW, D'Croz L (1990) Experimental evidence for high temperature stress as the cause of El Nino-coincident coral mortality. *Coral Reefs*, **8**, 181-191.

Hennige SJ, Wicks LC, Kamenos NA, Bakker DCE, Findlay HS, Dumousseaud C, Roberts JM (2014) Short-term metabolic and growth responses of the cold-water coral *Lophelia pertusa* to ocean acidification. *Deep-Sea Research II*, **99**, 27-35.

Hoegh-Guldberg O (1999) Climate change, coral bleaching and the future of the world's coral reefs. *Marine and Freshwater Research*, **50**, 839–866.

Hoegh-Guldberg O, Mumby PJ, Hooten AJ, Steneck RS, Greenfield P, Gomez E, Harvell CD, Sale PF, Edwards AJ, Caldeira K, Knowlton N, Eakin CM, Iglesias-Prieto R, Muthiga N, Bradbury RH, Dubi A, Hatziolos ME (2007) Coral reefs under rapid climate change and ocean acidification. *Science*, **318**, 1737-1742.

Holcomb M, Cohen AL, Gabitov RI, Hutter JH (2009) Compositional and morphological features of aragonite precipitated experimentally from seawater and biogenically by corals. *Geochemica et Cosmochimica Acta*, **73**, 4166-4179.

Holcomb M, McCorkle DC, Cohen AL (2010) Long-term effects of nutrient and CO_2 enrichment on the temperate coral *Astrangia poculata*. Journal of Experimental Marine Biology and Ecology, **386**, 27–33.

IPCC (2007) *Climate Change 2007: Summary for Policymakers of the Synthesis Report of the IPCC Fourth Assessment Report*. (eds. Metz B, Davidson OR, Bosch PR, Dave R, Meyer LA). 23 pp., Cambridge University Press, Cambridge, United Kingdom and New York, NY, USA.

IPCC (2007b) *Climate Change 2007: Synthesis Report, Contribution of Working Groups I, II and III to the Fourth Assessment Report of the Intergovernmental Panel on Climate Change*. (eds. Pachauri RK, Reisinger A), 104 pp., IPCC, Geneva, Switzerland.

Jokiel PL, Coles SL (1977) Effects of temperature on the mortality and growth of Hawaiian reef corals. *Marine Biology*, **43**, 201-208.

Jokiel PL, Rodgers KS, Kuffner, IB, Andersson, AJ, Cox EF, Mackenzie FT (2008) Ocean acidification and calcifying reef organisms: A mesocosm investigation. *Coral Reefs*, **27**, 473–483.

Jury CP, Whitehead RF, Szmant AM (2009) Effects of variations incarbonate chemistry on the calcification rates of *Madracis auretenra* (= *Madracis mirabilis sensu* Wells, 1973): bicarbonate concentrations best predict calcification rates. *Global Change Biology*, **16**, 1632–1644.

Keeling CD (1960) The concentration and isotopic abundances of carbon dioxide in the atmosphere. *Tellus*, **12**, 200–203.

Keeling RF, Piper SC, Bollenbacher AF, Walker JS (2009) Atmospheric CO_2 records from sites in the SIO air sampling network. In: *Trends: A Compendium of Data on Global Change.* Carbon Dioxide Information Analysis Center, Oak Ridge National Laboratory, U.S. Department of Energy, Oak Ridge, Tennessee, USA.

Kleypas JA, Feely RA, Fabry VJ, Langdon C, Sabine CS, Robbins LL (2006) *Impacts of ocean acidification on coral reefs and other marine calcifiers: A guide for future research - St Petersburg Report*, NSF, NOAA, and the US Geological Survey, St. Petersburg, FL.

Krief S, Hendy EJ, Fine M, Yam R, Meibom A, Foster GL, Shemesh A (2010) Physiological and isotopic responses of scleractinian corals to ocean acidification. *Geochimica et Cosmochimica Acta*, **74**, 4988–5001.

Kump LR, Bralower TJ, Ridgwell A (2009) Ocean acidification in deep time. *Oceanography*, **22**, 94–107.

Langdon C, Takahashi T, Sweeney C, Chipman D, Goddard J, Marubini F, Aceves H, Barnett H, Atkinson MJ (2000) Effect of calcium carbonate satyration state on the calcification rate of an experimental coral reef. *Global Biogeochemical Cycles*, **14**, 639-654.

Langdon C (2002) Review of experimental evidence for effects of CO_2 on calcification of reef-builders. *Proceedings of the Ninth International Coral Reef Symposium*, 1091-1098.

Langdon C, Atkinson MJ (2005) Effect of elevated pCO_2 on photosynthesis and calcification of corals and interactions with seasonal change in temperature/irradiance and nutrient enrichment. *Journal of Geophysical Research*, **110**, C09S07, doi:10.1029/2004JC002576.

Leclercq N, Gattuso JP, Jaubert J (2002) Primary production, respiration, and calcification of a coral reef mesocosm under increased CO_2 partial pressure. *Limnology and Oceanography*, **47**, 558–564.

Lewis E, Wallace DWR (1998) *CO2SYS: Program developed for CO_2 system calculations*, Carbon Dioxide Information Analysis Center, Oak Ridge National Laboratory, U.S. Department of Energy, Oak Ridge, Tennessee.

Lough JM, Barnes D J (2000) Environmental controls on growth of the massive coral Porites. *Journal of Experimental Marine Biology and Ecology*, **245**, 225-243, doi:10.1016/s0022-0981(99)00168-9.

Luthi D, Le Floch M, Bereiter B, Blunier T, Barnola JM, Siegenthaler U, Raynaud D, Jouzel J, Fischer H, Kawamura K, Stocker TF (2008) High-resolution carbon dioxide concentration record 650,000–800,000 years before present. *Nature*, **453**, 379–382.

Maier C, Watremez P, Taviani M, Weinbauer MG, Gattuso JP (2011) Calcification rates and the effect of ocean acidification on Mediterranean cold-water corals. *Proceedings of the Royal Society B*, **279**, 1713–1723 doi: 10.1098/rspb.2011.1763.

Maier C, Schubert A, Berzunza Sànchez MM, Weinbauer MG, Watremez P, Gattuso JP (2013) End of the century pCO_2 levels do not impact calcification in Mediterranean cold-water corals. *PLoS ONE*, **8**, e62655. doi:10.1371/journal.pone.0062655.

Marubini F, Barnett H, Langdon C, Atkinson M (2001) Dependence of calcification on light and carbonate ion concentration for the hermatypic coral Porites compressa. *Marine Ecology Progress Series*, **220**, 153–162.

Marubini F, Ferrier-Pages C, Cuif JP (2003) Suppression of skeletal growth in scleractinian corals by decreasing ambient carbonate-ion concentration: a crossfamily comparison. *Proceedings of the Royal Society of London B*, **270**, 179–184.

McCulloch M, Falter J, Trotter J, Montagna P (2012) Coral resilience to ocean acidification and global warming through pH up-regulation. *Nature Climate Change*, **2**, 623-627.

McNeil BI, Matear RJ, Barnes DJ (2004) Coral reef calcification and climate change: The effect of ocean warming. *Geophysical Research Letters*, **31**, L22309.

Movilla J, Calvo E, Pelejero C, Coma R, Serrano E, Fernandez-Vallejo P, Ribes M (2012) Calcification reduction and recovery in native and non-native Mediterranean corals in response to ocean acidification. *Journal of Experimental Marine Biology and Ecology*, **438**, 144-153.

Mucci A (1983) The solubility of calcite and aragonite in seawater at various salinities, temperatures, and one atmosphere total pressure. *American Journal of Science*, **283**, 780–799.

Muehllehner N, Edmunds PJ (2008) Effects of ocean acidification and increased temperature on skeletal growth of two scleractinian coals, *Pocillopora meandrina* and *Porites rus*. *Proceedings of the 11th International Coral Reef Symposium, Ft. Lauderdale*, **3**, 57-61.

Neftel A, Moor E, Oeschger H, Stauffer B (1985) Evidence from polar ice cores for the increase in atmospheric CO_2 in the past two centuries. *Nature*, **315**, 45–47.

Nie B, Chen T, Liang M, Wang Y, Zhong J, Zhu Y (1997) Relationship between coral growth rate and sea surface temperature in the northern part of South China Sea during the past 100 a. Science in China Series D. *Earth Sciences*, **40**, 173-182.

Ohki S, Irie T, Inoue M, Shinmen K, Kawahata H, Nakamura T, Kato A, Nojiri Y, Suzuki A, Sakai K, van Woesik R (2013) Calcification responses of symbiotic and aposymbiotic corals to near-future levels of ocean acidification. *Biogeosciences*, **10**, 6807-6814.

Orr JC, Fabry VJ, Aumont O, Bopp L, Doney SC, Feely RA, Gnanadesikan A, Gruber N, Ishida A, Joos F, Key RM, Lindsay K, Maier-Reimer E, Matear R, Monfray P, Mouchet A, Najjar RG, Plattner G, Rodgers KB, Sabine CL, Sarmiento JL, Schlitzer R, Slater RD, Totterdell IJ, Weirig M, Yamanaka Y, Yool A (2005) Anthropogenic ocean acidification over the twenty-first century and its impact on calcifying organisms. *Nature*, **437**, 681-686, doi:10.1038/nature04095.

Rahmstorf S, Cazenave A, Church JA, Hansen JE, Keeling RF, Parker DE, Somerville RCJ (2007) Recent climate observations compared to projections. *Science*, **316**, 709.

Raven J, Caldeira K, Elderfield H, Hoegh-Guldberg O, Liss P, Riebesell U, Shepherd J, Turley C, Watson A (2005) *Ocean acidification due to increasing atmospheric carbon dioxide*, The Royal Society, London.

Reynaud S, Leclercq N, Romaine-Lioud S, Ferrier-Pagès C, Jaubert J, Gattuso JP (2003) Interacting effects of CO_2 partial pressure and temperature on photosynthesis and calcification in a scleractinian coral. *Global Change Biology*, **9**, 1660-1668.

Riebesell U, Fabry V J, Hansson L, Gattuso JP (2010) *Guide to best practices for ocean acidification research and data reporting*, Publications Office of the European Union, Luxembourg.

Ries JB, Cohen, AL, McCorkle DC (2009) Marine calcifiers exhibit mixed responses to CO_2-induced ocean acidification. *Geology*, **37**, 1131-1134.

Ries JB, Cohen AL, McCorkle DC (2010) A nonlinear calcification response to CO_2-induced ocean acidification by the coral Oculina arbuscula. *Coral Reefs*, **29**, 661-674.

Ries JB (2011) A physicochemical framework for interpreting the biological calcification response to CO_2-induced ocean acidification. *Geochimica et Cosmochimica Acta*, **75**, 4053-4064.

Rodolfo-Metalpa R, Martin S, Ferrier-Pagès C, Gattuso JP (2010) Response of the temperate coral Cladocora caespitosa to mid- and long-term exposure to pCO_2 and temperature levels projected for the year 2100. *Biogeosciences*, **7**, 289-300.

Rodolfo-Metalpa R, Houlbreque F, Tambutte E, Boisson F, Baggini C, Patti FP, Jeffree R, Fine M, Foggo A, Gattuso JP, Hall-Spencer JM (2011) Coral and mollusk resistance to ocean acidification adversely affected by warming. *Nature Climate Change*, **1**, 308–312.

Roy RN, Roy LN, Vogel KM, Porter-Moore C, Pearson T, Good CE, Millero FJ, Campbell DM (1993) The dissociation constants of carbonic acid in seawater at salinities 5 to 45 and temperatures 0 to 45 °C. *Marine Chemistry*, **44**, 249–267.

Schneider K, Erez J (2006) The effect of carbonate chemistry on calcification and photosynthesis in the hermatypic coral Acropora eurystoma. *Limnology and Oceanography*, **51**, 1284–1295.

Schoepf V, Grottoli AG, Warner ME, Cai WJ, Melman TF, Hoadley KD, Pettay DT, Hu X, Li Q, Xu H, Wang Y, Matsui Y, Baumann JH (2013) Coral Energy Reserves and Calcification in a high- CO_2 world at two temperatures. *PLoS ONE*, **8**, 1-11.

Siebeck UE, Marshall NJ, Klüter A, Hoegh-Guldberg O (2006) Monitoring coral bleaching using a colour reference card. *Coral Reefs*, **25**, 453-460.

Singmann H, Bolker B, Højsgaard S, Fox M, Lawrence MA, Mertens, U (2014). Package 'afex'. Retrieved from http://r-mirror.de/web/packages/afex/afex.pdf.

Tanzil JTI, Brown BE, Tudhope AW, Dunne RP (2009) Decline in skeletal growth of the coral *Porites* lutea from the Andaman Sea, South Thailand between 1984 and 2005. *Coral* reefs, 28, 519-528.

Tans P, Keeling R NOAA/ESRL (www.esrl.noaa.gov/gmd/ccgg/trends/) and Dr. Ralph Keeling, Scripps Institution of Oceanography (scrippsco2.ucsd.edu/).

Trotter J, Montagna P, McCulloch M, Silenzi S, Reynaud S, Mortimer G, Martin S, Ferrier-Pagès C, Gattuso JP, Rodolpho-Metalpa R (2011) Quantifying the pH 'vital effect' in the temperate zooxanthellate coral *Cladocora caespitosa*: Validation of the boron seawater pH proxy. *Earth and Planetary Science Letters*, **303**, 163–173.

Venn AA, Tambutté E, Holcomb M, Laurent J, Allemand D, Tambutté S (2012) Impact of seawater acidification on pH at the tissue–skeleton interface and calcification in reef corals. *Proceedings of the National Academy of Sciences*, **110**, 1634–1639.

Veron AT (1993) *Corals of Australia and the Indo-Pacific*, University of Hawaii Press, Honolulu.

Worrell E, Price L, Martin N, Hendriks C, Meida LO (2001) Carbon dioxide emissions from the global cement industry. *Annual Review of Energy and the Environment*, **26**, 303–329.

Zeebe RE, Wolf-Gladrow D (2001) *CO_2 in Seawater: Equilibrium, Kinetics, Isotopes*, Elsevier Oceanography Series 65, Amsterdam.